

CHEHAB RL: Learning to Optimize Fully Homomorphic Encryption Computations

Bilel Sefsaf

New York University Abu Dhabi
Abu Dhabi, United Arab Emirates
Ecole Superieure d’Informatique
Algiers, Algeria
kb_sefsaf@esi.dz

Arab Mohammed

New York University Abu Dhabi
Abu Dhabi, United Arab Emirates
Ecole Superieure d’Informatique
Algiers, Algeria
km_arab@esi.dz

Abderraouf Dandani

New York University Abu Dhabi
Abu Dhabi, United Arab Emirates
Ecole Superieure d’Informatique
Algiers, Algeria
ka_dandani@esi.dz

Eduardo Chielle

Center for Cyber Security
New York University Abu Dhabi
Abu Dhabi, United Arab Emirates
ec126@nyu.edu

Riyadh Baghdadi

New York University Abu Dhabi
Abu Dhabi, United Arab Emirates
rb4792@nyu.edu

Abdessamed Seddiki

New York University Abu Dhabi
Abu Dhabi, United Arab Emirates
Ecole Superieure d’Informatique
Algiers, Algeria
ka_seddiki@esi.dz

Michail Maniatakos

Center for Cyber Security
New York University Abu Dhabi
Abu Dhabi, United Arab Emirates
mm6446@nyu.edu

Abstract

Fully Homomorphic Encryption (FHE) enables computations directly on encrypted data, but its high computational cost remains a significant barrier. Writing efficient FHE code is a complex task requiring cryptographic expertise, and finding the optimal sequence of program transformations is often intractable. In this paper, we propose CHEHAB RL, a novel framework that leverages deep reinforcement learning (RL) to automate FHE code optimization. Instead of relying on predefined heuristics or combinatorial search, our method trains an RL agent to learn an effective policy for applying a sequence of rewriting rules to automatically vectorize scalar FHE code while reducing instruction latency and noise growth. The proposed approach supports the optimization of both structured and unstructured code. To train the agent, we synthesize a diverse dataset of computations using a large language model (LLM). We integrate our proposed approach into the CHEHAB FHE compiler and evaluate it on a suite of benchmarks, comparing its performance against Coyote, a state-of-the-art vectorizing FHE compiler. The results show that our approach generates code that is $5.3\times$ faster in execution, accumulates $2.54\times$ less noise, while the compilation process itself is $27.9\times$ faster than Coyote (geometric means).

CCS Concepts: • Software and its engineering → Compilers.

Keywords: Automatic Code Optimization, Compiler, FHE, Fully Homomorphic Encryption, Reinforcement Learning

1 Introduction

In Fully Homomorphic Encryption (FHE), computations are performed directly on encrypted data without decryption. This enables a client to transmit data to a third party that processes it and returns the result without performing decryption. As a result, sensitive information remains protected.

Despite notable recent progress and increasing practical adoption [35, 41, 46, 48, 72], FHE remains computationally expensive. For example, a ciphertext¹ multiplication takes 10^6 times longer than its plaintext counterpart². This disparity is due to the inherent complexity of homomorphic operations, as a single ciphertext multiplication entails multiple n -order polynomial multiplications. Reducing the execution time of FHE applications is essential for their practical adoption. Consequently, experts devote substantial effort to optimizing FHE implementations.

Writing efficient code for FHE is tedious, though. It requires a considerable amount of expertise in writing low-level code for the target scheme. This makes writing code for FHE applications time-consuming and error-prone and hinders its wide adoption [21, 72]. To address this problem, the research community has explored the development of compilers for FHE applications [21, 23, 26, 27, 49, 52, 72]. HECO [72], for example, focuses on efficiently transforming



This work is licensed under a Creative Commons Attribution 4.0 International License.

¹Ciphertext: encrypted data; Plaintext: clear data.

²Evaluation done on the BFV scheme, for 128-bit security, using Microsoft SEAL [57] and running on a modern multicore CPU.

structured code into the FHE paradigm with SIMD instructions (structured code, a.k.a. regular code, stands for code with loops). In a similar way, CHET [27] focuses on the vectorization of structured computations over packed tensors (such as neural networks). However, neither of these compilers supports vectorizing unstructured code (arbitrary, non-loop-based code).

More recent work, such as Coyote [52] and Porcupine [23], proposes compilers that support vectorization of both structured and unstructured code. However, both Coyote and Porcupine frame vectorization as search over a combinatorial design space: which subexpressions to pack, how to lay out data in wide ciphertext vectors, where to insert rotations and masks, etc. In such a complex space, local choices have non-local effects (e.g., a packing decision can increase later rotations or depth), so simple heuristics or greedy rule application often get trapped in poor local optima. To mitigate this, Coyote couples hand-tuned heuristics with an ILP solver to select packs, while Porcupine uses program synthesis to enumerate and check candidates [23, 52]. These strategies are effective, but they are limited in their scalability: exploring or solving over large candidate sets becomes computationally expensive as programs grow in size.

In this paper, we argue that Reinforcement Learning (RL) provides a better solution: we treat FHE code optimization as sequential decision-making and use RL to learn a policy that composes sequences of rewriting rules to minimize latency and noise. By optimizing a single global cost, the RL policy makes global decisions without explicit combinatorial enumeration or ILP, yielding high-quality transformations with substantially lower compile time.

More concretely, we propose CHEHAB RL, a novel framework that leverages reinforcement learning (RL) to automatically optimize code for the field of FHE. It supports both structured and unstructured code and scales better than existing approaches. CHEHAB RL automatically vectorizes code while minimizing noise growth and circuit latency. This is achieved through a policy network that selects a sequence of rewriting rules to apply to code to vectorize it while minimizing rotations, circuit depth, multiplicative depth, and other FHE operations. Because our approach selects the sequence of rewriting rules using a policy network, it avoids computationally expensive search methods used in state-of-the-art FHE compilers, and therefore scales better.

Bringing RL into this setting is nontrivial and requires addressing several FHE-specific challenges: 1) Large action space. The agent chooses from an extensive set of rules, each applicable to multiple locations. This makes the action space large. To address this challenge, we propose a multi-discrete hierarchical policy supported by a position network where the agent first decides about which transformation to apply, then decides about where to apply it. We show that this design outperforms a flat action space. 2) Fast, FHE-aware reward. Running FHE code during training to obtain a reward

is prohibitively slow. To address this challenge, we introduce an analytical reward function tailored to the FHE domain. It combines operation cost, circuit depth, and multiplicative depth and captures both performance and noise growth, while enabling fast training. 3) LLM-Synthesized dataset. Since no dataset of optimizable FHE programs exists, we build an LLM-based synthesis pipeline and use it to generate data and show that training on this data yields much better agents than training on random programs.

We integrate our proposed approach into the CHEHAB FHE compiler and evaluate it on a set of kernels, comparing it to Coyote, a state-of-the-art FHE compiler, and demonstrate that it produces higher-quality code and scales better.

The contributions of the paper are as follows:

1. We formulate the problem of FHE code optimization as a sequential decision-making problem, and propose to learn a policy using RL to solve it.
2. We propose CHEHAB RL, a novel framework that leverages RL to automatically vectorize structured and unstructured FHE code and minimize noise growth and circuit latency while scaling better compared to state-of-the-art. To the best of our knowledge, this is the first use of RL to solve this problem.
3. We use an LLM-guided synthesis pipeline to generate a large training dataset of FHE expressions (15,855 expressions), and show that training on this dataset outperforms training on randomly generated FHE expressions.
4. We compare CHEHAB RL to Coyote and show that it generates code that is 5.3× faster, accumulates 2.54× less noise, while it takes 27.9× less time in compilation.
5. We release CHEHAB RL to the community³.

2 Motivating Example

Vectorization in FHE is challenging as it introduces rotations, masking, and data packing. Poor vectorization can increase the number of rotations and circuit depth, severely impacting performance and increasing noise in the circuit. Thus, effective FHE vectorization must maximize code vectorization while minimizing rotation overhead and circuit depth.

Consider this unstructured (non-loop-based) code:

$$x = (((v_1 \cdot v_2) \cdot (v_3 \cdot v_4)) + ((v_3 \cdot v_4) \cdot (v_5 \cdot v_6))) \cdot ((v_7 \cdot v_8) \cdot (v_9 \cdot v_{10})) \quad (1)$$

Fig. 1 represents the code as a circuit (a common representation of code in the FHE literature). This expression is not trivial to vectorize.

To vectorize it, we use a Term Rewriting System (TRS) consisting of a set of rules. For illustration, we show only three rules, but the TRS has more.

R1: multiplication_commutativity, $a \cdot b \Rightarrow b \cdot a$

R2: comm_factor, $a \cdot b + a \cdot c \Rightarrow a \cdot (b + c)$

R3: vectorization, $(a \cdot b) + (c \cdot d) \Rightarrow \text{Vec}(a, c) \cdot \text{Vec}(b, d)$

³<https://github.com/Modern-Compilers-Lab/CHEHAB>

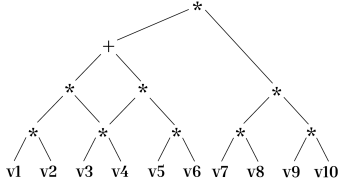


Figure 1. Example of an unstructured scalar code.

	$[1, 2, 3] = [v_1, v_5, v_6] \cdot [v_2, 1, 1]$
$[1, 2] = [v_1, v_5] \cdot [v_2, v_6]$	$[4, _] = [2, _] \cdot [3, _]$
$[3, _] = [1, _] + [2, _]$	$[5, _] = [1, _] + [4, _]$
$[4, _] = [v_3, _] \cdot [v_4, _]$	$[6, _] = [v_3, _] \cdot [v_4, _]$
$[5, _] = [3, _] \cdot [4, _]$	$[7, _] = [5, _] \cdot [6, _]$
$[6, 7] = [v_7, v_9] \cdot [v_8, v_{10}]$	$[8, 9, _] = [v_7, v_9, _] \cdot [v_8, v_{10}, _]$
$[8, _] = [6, _] \cdot [7, _]$	$[10, _] = [8, _] \cdot [9, _]$
$[x, _] = [5, _] \cdot [8, _]$	$[x, _] = [7, _] \cdot [10, _]$
(a) First approach.	(b) Second approach.

Figure 2. Vectorization approaches.

We first apply the rules R1 then R2, yielding:

$$x = ((v_3 \cdot v_4) \cdot ((v_1 \cdot v_2) + (v_5 \cdot v_6))) \cdot ((v_7 \cdot v_8) \cdot (v_9 \cdot v_{10})) \quad (2)$$

From this transformed expression, we can apply other rewriting rules to vectorize the code. There are many ways to vectorize it (also called vectorization strategies). We show two examples in Fig. 2 (intermediate values are named using numbers). Each vectorization strategy is obtained by applying a different sequence of rewriting rules. The key challenge is determining the sequence of rewriting rules that yields the best vectorization strategy while minimizing the number of rotations and depth of the circuit (multiplicative depth, more precisely, as we illustrate later).

We omit showing the rotation and masking instructions in the example for brevity. For example, in Fig. 2a, in order to calculate the operands of the 2nd statement ($[1, _]$ and $[2, _]$), rotations and masking should be applied on the result of the 1st statement as follows⁴:

$$\begin{aligned} [1, _] &= [1, 2] \& [F, _] \\ [2, _] &= ([1, 2] \ll 1) \& [F, _] \end{aligned}$$

but we omit showing these rotations and maskings.

Let us compare the two vectorizations in Fig. 2 using an approximate cost model that assigns a relative latency to each operation: multiplications and rotations have a latency of 1, while additions have a latency of 0.1 (these values are toy values chosen for simplicity only, to illustrate the example). The original scalar expression has 9 multiplications and 1 addition, yielding a total cost of 9.1. The vectorization in Fig. 2a reduces the number of multiplications to 6 and additions to 1 but introduces 2 rotations, resulting in a total cost of 8.1. In contrast, the vectorization in Fig. 2b involves 7

⁴We assume 4-bit numbers in the example for simplicity, and we use $_$ to denote a zero-valued slot.

multiplications, 3 rotations, and 1 addition, yielding a 10.1 cost.

These results highlight that not all vectorizations are equally beneficial. Moreover, applying R1 prior to R2 is essential to obtain the expression in Eq. 2, which can then be vectorized by applying R3. In contrast, starting with R2 followed by R1 yields Eq. 1, where R3 is no longer applicable, thereby eliminating vectorization opportunities. This limitation highlights the importance of carefully selecting which rules to apply and in which order. To address this, we employ a policy network, trained via RL. The policy determines an ordered sequence of rules that optimize the code to achieve the best global vectorization, rather than relying on local improvements alone.

Vectorization in FHE. Vectorization in FHE is different from classical vectorization. While many code vectorization methods have been studied in the literature [10, 12, 19, 45, 47, 53, 68], such methods are not well-suited for vectorizing FHE code. First, since FHE does not support loops or conditionals, computations must be expressed as arithmetic circuits (unstructured code), preventing the direct use of classical loop-based vectorization methods. FHE vectorization differs from classical SLP-based approaches (Superword-level parallelism) [19, 47, 53] due to the large vector sizes in FHE (thousands of slots vs a few in hardware registers) and the inability to index ciphertext vectors directly. Instead, expensive rotation operations simulate indexed accesses. In addition, rotations in FHE are computationally expensive and increase noise in the circuit, so vectorization strategies must minimize their use. These differences make classical SLP-based methods unsuitable for FHE, as we discuss in Sec. 8. Because ciphertext vectors are wider in FHE compared to traditional hardware vector registers, FHE vectorization yields significant speedups because a single ciphertext operation (add or multiply) applies element-wise to every packed slot in the ciphertext, so one operation can replace thousands of scalar steps, far beyond the 4–8-lane limits of hardware SIMD.

3 Background

3.1 Fully Homomorphic Encryption

FHE allows computations on encrypted data directly (i.e., without decrypting the data). For a function f and a message m , FHE allows the possibility of computing $\hat{y} = f(\hat{m})$, without knowing m . Here, \hat{m} represents the encryption of m , and \hat{y} is the encrypted output, which must be decrypted by the owner of m to obtain the output $\hat{y} \mapsto y$ in plaintext. FHE hence helps to achieve privacy-preserving computation in situations where sensitive data needs to be shared with third parties for computation offloading.

The Brakerski/Fan-Vercauteren (BFV) encryption scheme [14, 32] is an FHE scheme that provides primitives for modular addition and multiplication along with primitives for

noise management and ciphertext maintenance (i.e., relinearization, modulus switching, and bootstrapping). BFV operates within plaintext and ciphertext spaces. Plaintexts and ciphertexts are large order polynomials defined by the parameters $\{n, t, q\}$. The degree n corresponds to the polynomial modulus $x^n + 1$, while the parameters t and q are the plaintext modulus and ciphertext modulus.

Encryption introduces *noise* for security, which grows with operations on ciphertexts or between a ciphertext and a plaintext. Its growth is limited by q and t (defined in A.2.1); exceeding this limit corrupts the data, leading to incorrect decryption (a user sets a noise budget for their circuit, and the circuit has to run without exceeding that noise budget). *Bootstrapping* can reset noise but has high computational costs. Instead, FHE applications typically limit operations to a predefined depth. Supporting deeper circuits requires increasing q and adjusting n for security. This is especially important for circuits with high multiplicative depth, as multiplications cause exponential noise growth, while additions increase it linearly. However, larger q and n also introduce performance overheads due to larger polynomials and coefficients. Therefore, one of the goals when optimizing an FHE circuit is to minimize the multiplicative depth to be able to use the smallest q and n that still respect the noise budget in the circuit. This, in turn, makes FHE operations run faster and reduces the overall circuit latency.

Vectorization in FHE (a.k.a., *batching*) is a technique that encodes a vector of n integers in a single plaintext polynomial using the Chinese Remainder Theorem (CRT). Vectors in FHE are large (thousands of slots). With vectorization, additions and multiplications are executed slot-wise in a Single-Instruction Multiple-Data (SIMD) fashion. Moreover, BFV supports rotations of the encoded vector to move data (and perform data packing). Rotation as a function takes a ciphertext (vector) and a rotation step and returns the ciphertext (vector) with slots shifted in a cyclic manner. For example, the rotation $[1, 2, 3] \lll 1$ returns $[2, 3, 1]$. Note that FHE supports only additions, multiplications, and rotations and does not support branches or loops. See Appendix A.2 for a formal definition of FHE concepts.

3.1.1 Circuit Depth and Multiplicative Depth.

Circuit Depth. An FHE program can also be represented as a circuit. A circuit is a DAG (Directed Acyclic Graph) representation of the program that captures its dataflow. Calculating the depth of the circuit is important for estimating noise. The depth of a circuit (DAG) represents the maximum number of consecutive operations performed on an input to compute the output. The depth of a node v in the DAG is defined as the length of the longest path between v and an input node. This depth is usually used to quantify the noise in the circuit. However, it does not provide any information on the type of operations involved (which is necessary to determine how the noise grows). Since multiplication has the

most significant impact on noise, one should compute the multiplicative depth of the circuit to estimate noise better.

Multiplicative Depth of a Circuit. Similar to circuit depth, except that we consider counting the number of multiplications only, since multiplications increase noise exponentially. The multiplicative depth of a node v is defined as the length of the longest path, when counting multiplication operations alone, between v and an input node.

4 CHEHAB RL Overview

This section provides an overview of CHEHAB RL and its components. We first show the overall design of the CHEHAB compiler and then discuss its major components, including our RL agent for code optimization. CHEHAB defines a domain-specific language (DSL) for FHE. The CHEHAB DSL is the compiler’s starting point. An intermediate representation (IR) is first generated from the CHEHAB DSL. This IR is then optimized by a Reinforcement learning (RL) agent, which learns a policy to apply a sequence of transformations. These transformations are drawn from a set of rewriting rules that include rules for both code vectorization and for simplification to reduce noise growth and instruction latency (i.e., rewrite complex arithmetic expressions into simpler expressions that have a smaller number of operations and depth). Next, the compiler performs the rotation key selection. This pass generates the necessary rotation keys for rotation operations found in the optimized code. Finally, the code generator generates a sequence of vectorized operations implemented in C++ and targeting Microsoft SEAL’s backend [57] for BFV. The key new contribution introduced by this paper is CHEHAB RL, the RL-guided term rewriting system, which we integrate into the CHEHAB compiler as shown in Fig. 3. We present the RL agent in detail in the paper, while we present the rotation key selection method in Appendix B.

4.1 CHEHAB Domain Specific Language (DSL)

FHE performance and correctness critically depend on managing the encryption parameters and rotation keys. Managing these keys and parameters manually is a time-consuming task that requires expertise. The CHEHAB DSL is designed to manage this complexity automatically, and thus improves the productivity of the developer. The developer expresses their code using a simple, high-level C++ code, while CHEHAB takes care of lowering that code to the FHE paradigm and takes care of generating and managing all the FHE-related objects (such as the encryption keys). CHEHAB is embedded in C++, allowing users to leverage C++ features (e.g., templates) while extending it by defining the Plaintext and Ciphertext types. It also overloads basic operations for these types, mapping them to native FHE operations. One of the guiding principles in designing CHEHAB is the clear separation between computations and implementation details. In

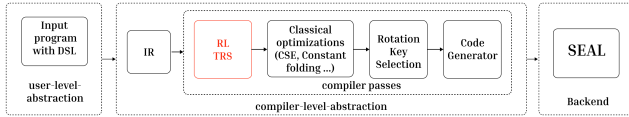


Figure 3. CHEHAB RL overview (our contribution: *RL TRS*).

particular, it allows computations to be specified independently from encryption parameters, offering greater flexibility in exploiting potential optimization opportunities.

A program written in CHEHAB has three parts: (1) Input declaration: This section defines the inputs of the program. An input can be either a ciphertext or a plaintext. It can also be either a scalar or a vector. (2) Computations: This section specifies the computations, whether arithmetic or rotation operations, using standard C++ operators (+, -, *, «). These operators are mapped to either vector or scalar operators depending on the type of their operands. (3) Outputs: This section declares the outputs.

The following example shows how to express the motivating example in our DSL. The list of operations supported by CHEHAB is presented in Table 3 in the appendix.

```

Ciphertext motivating_example() {
  Ciphertext v1, v2, v3, v4, v5, v6, v7, v8, v9, v10; //Inputs
  Ciphertext x = (((v1 * v2) * (v3 * v4)) + ((v3 * v4) *
(v5 * v6))) * ((v7 * v8) * (v9 * v10)); //Computations
  x.set_output(); //Outputs
  return x;
}
  
```

4.2 CHEHAB Intermediate Representation (IR)

The DSL program is compiled into an intermediate representation (IR) in the form of an AST (Abstract Syntax Tree), as is commonly done in compilers. Fig. 1 shows an example of an AST representation of the motivating example. From this representation, we extract a dataflow graph representation (DAG) of the code when needed (e.g., to calculate the multiplicative depth). To lower the DSL to the IR, we follow the same approach of Halide [62] and Tiramisu [10]. The approach relies on the use of templates and staging in C++.

4.3 Code Optimizations

After generating the IR, the next stage is code optimization. CHEHAB RL uses an RL agent to optimize code. The agent chooses a sequence of rules from its rule set. This set includes rules for *vectorization*, which group scalar operations into vector ones, and rules for *simplification*, which minimize noise growth and latency in the circuit. To further optimize code, the original CHEHAB compiler applies classic compiler optimizations, including common subexpression elimination (CSE), constant folding, and dead code elimination.

4.4 Code generation

In the final stage, CHEHAB generates code that targets the SEAL API [57] by mapping each node in the IR (operator) to its equivalent API call in SEAL. During code generation, we also generate the necessary masking operations, private keys,

public keys, and relinearization keys. More details about code generation in Appendix D.

5 FHE Circuit Optimization

The core of the CHEHAB RL framework is a Term Rewriting System (TRS) that uses RL to transform an initial Intermediate Representation (IR) into an efficient one. We frame the optimization task as a sequential decision-making problem, formally a Markov Decision Process (MDP).

Our RL framework uses the actor-critic RL architecture and is defined by the following key components: 1) *State representation* (detailed in Sec. 5.1): provides a representation of the program being optimized; 2) *Action space* (Sec. 5.2): defines the set of rewriting rules that the agent can apply to the program being optimized; 3) *Reward model* (Sec. 5.3): provides a function that scores the quality of actions, guiding the agent toward actions that produce FHE circuits that are more efficient and have less noise; 4) *Actor-critic networks* (Sec. 5.4): the actor selects the next rewriting rule to apply given the current program state, and selects where to apply it, while the critic estimates the expected return and provides the learning signal for policy optimization during training (the critic is only used during training to train the policy).

We train our proposed RL agent on an *LLM-generated dataset* (described in Sec. 6) using the *PPO learning algorithm* (Sec. 7.1). The following sections describe these components.

5.1 State Representation

The goal of the state representation is to produce a fixed-length vector embedding, s_P , that represents a given program IR, P . To extract the program representation, we first tokenize the program being optimized. We use a simple method that we call *Identifier and Constant Invariant (ICI)* tokenization. Conceptually, ICI is a form of *alpha-renaming* [2] combined with simple program canonicalization. ICI produces a canonical token sequence that is invariant to identifier names and to the concrete values of constants. For each program P , we rename variables such that the first distinct variable is mapped to v_0 , the second to v_1 , and so on. For example, the two semantically equivalent expressions $(+ a (+ b c))$ and $(+ x (+ y z))$ are both mapped to the exact same canonical sequence: $(+ v_0 (+ v_1 v_2))$. This normalization has a few practical benefits for learning: (i) it collapses programs that differ only by identifier naming or by value-agnostic constants into the same representation, reducing the effective vocabulary and simplifying generalization; (ii) it produces a stable canonical form that we reuse for dataset deduplication, avoiding redundant near-duplicate training samples; (iii) ICI tokenization is computationally lightweight: it is a single linear scan with $O(1)$ expected-time hash map operations per new symbol. This contrasts with learned subword tokenizers such as Byte Pair Encoding (BPE) [65], which repeatedly

applies merge rules and performs large-vocabulary prefix searches, adding nontrivial overhead.

More precisely, ICI uses a small fixed vocabulary for IR operators (e.g., +, *, VecAdd) and delimiters/parentheses, and builds per-program hash maps for identifiers and constants in a single left-to-right pass. For each program P , the first distinct variable is mapped to $v0$, the second to $v1$, and so on. Numerical constants are mapped similarly to $c0, c1, \dots$ with one important exception: the integers **0** and **1** are kept as literal tokens because they play a special semantic role in many rewrite rules (additive/multiplicative identities). For all other constants, we discard the literal value but preserve (i) that the token is a constant and (ii) whether two constant occurrences in the same expression are equal (e.g., the same constant reused in multiple positions receives the same $c\#$ token). This is sufficient for our term-rewriting system because our rewrite rules do not branch on specific numeric values beyond special cases such as 0/1. In practice, programs that differ only in identifier names or non-(0/1) constant values are typically optimized by the same rewrite strategy.

After tokenization, the program P is represented by a variable-length sequence of tokens, $T(P) = [t_1, t_2, \dots, t_k]$. We then convert this sequence into a fixed-length vector that captures the long-range dependencies and hierarchical structure implied by the tokens. For this, we use a Transformer encoder [70] that learns automatically a short, fixed-length embedding for the tokenized program. We chose this architecture because its self-attention mechanism is designed to model long-distance dependencies inherent in source code, a capability validated by state-of-the-art code models such as CodeBERT [33]. This is critical for processing the long token sequences that represent unrolled FHE programs. Early in the project, we compared the Transformer architecture to recurrent architectures, including LSTMs and GRUs, but they did not provide satisfactory results. The Transformer encoder follows a standard architecture, consisting of a stack of 4 identical layers. Each layer employs a multi-head attention mechanism with 8 attention heads. The input token embeddings are summed with absolute positional encodings to preserve sequence order, and the encoder processes this sequence to generate a 256-dimensional vector for each token (we use the CLS special token as a placeholder to summarize the entire input sequence, as is commonly done in the literature [28]).

5.2 Action Space

The action space defines the set of valid transformations the agent can perform on the current program state. In our framework, an action corresponds to a rewriting rule selected from a set of predefined rewriting rules.

A challenge in designing the action space is handling the location of rule application. A single rule might match multiple sub-expressions within the IR. To address this, the agent needs to select both a rule and a location. To enable

this, we propose a hierarchical action space composed of two steps: the agent first picks a rule to apply, then picks the location where to apply it. To implement this, we propose a *rule selection network* used to pick an action, and a *location selection network* used to pick a location. We compare this hierarchical formulation to a flat rule/location action space in Sec. 7.6, and show that the hierarchical agent learns faster and achieves higher average rewards in training compared to a flat action space (Fig. 13).

To allow the agent to control the length of the optimization process, the action space also includes a special *END* action. Selecting this action terminates the current optimization episode, allowing the agent to learn not only which rules to apply, but also when to stop.

In total, our TRS consists of 84 rewrite rules, in addition to the END action. To design these rules, we began by collecting rules from Halide’s TRS [58, 62], and excluded rules that are not compatible with FHE (comparison, division, etc.). We then added new rules designed to reduce circuit depth, multiplicative depth, rotations, and the total number of operations. More details about the rewriting rules in Appendix E.

5.3 Reward Model

The agent learns via a reward signal designed to guide it toward producing FHE circuits that have minimal latency and noise. This signal is derived from an FHE-aware cost function that evaluates the quality of a given IR. We will first show the cost function, and then show how it is used to compute the reward.

5.3.1 FHE Cost Function. The goal of this cost function is to capture the metrics that we aim to minimize: number of FHE operations, multiplicative depth, and depth of the circuit. We also want to minimize the use of scalar operations in favor of vector operations. By minimizing the previous metrics, we minimize latency and noise. To achieve our goal, we define the cost function of an IR expression, e , as the weighted sum of the metrics that we want to minimize:

$$\text{Cost}(e) = w_{\text{ops}} \cdot C_{\text{ops}}(e) + w_{\text{depth}} \cdot D_{\text{circuit}}(e) + w_{\text{mult}} \cdot D_{\text{mult}}(e)$$

Where C_{ops} is the cost of operations, D_{circuit} is its circuit depth, and D_{mult} is its multiplicative depth. The weights w_{ops} , w_{depth} , and w_{mult} reflect the importance of each metric in the cost function. For our experiments, we set all weights to 1. We study sensitivity to these weights in Sec. 7.6 and show that this configuration enables the RL agent to generate code that has minimal execution time. The components of the cost function are defined below.

Operations Cost (C_{ops}): This term quantifies the computational cost of all of the operators used in the expression. We assign a numerical cost to each operator. These numerical costs reflect its relative performance compared to other operators in the BFV scheme. The relative order of these operations is guided by former empirical studies on the cost

of FHE operations [43]. The costs are structured to incentivize vectorization: 1) *Vector Additions/Subtractions*: These have the lowest cost (1), as they represent the most efficient parallel operations. 2) *Vector Multiplications*: These have a higher cost than vector additions/subtractions, and usually cost 100× the cost of vector additions, and therefore we assign a cost of (100) to them. 3) *Rotations (<<)*: Rotations typically have a cost that is 0.5× to 1× of the cost of a vector multiplication (depending on the parameters). We assign a cost of (50) to rotations, reflecting that rotations might be cheaper than multiplications but always more expensive than additions. This incentivizes rotations over multiplications, since they have a cost that is usually less than or equal to the cost of multiplications. 4) *Scalar Operations (+, -, *)*: These are assigned a high cost (250) to reflect their inefficiency. While in this particular case, the value 250 is not derived empirically, we chose this high cost for scalar operations to incentivize the RL to generate vectorized code.

The total C_{ops} is the sum of the costs of all the nodes in the expression tree.

Circuit Depth (D_{circuit}). A greater depth implies more sequential operations are performed on a ciphertext, which leads to a larger accumulation of noise. Minimizing depth is therefore critical, as it directly impacts the noise.

Multiplicative Depth (D_{mult}). This metric is critical as noise growth in the BFV scheme is directly proportional to the multiplicative depth. Therefore, to minimize the noise, we aim to minimize the multiplicative depth.

The three terms have different numerical ranges: C_{ops} can be in the hundreds, while D_{circuit} and D_{mult} are typically in the single digits. As a result, even with equal weights the objective tends to prioritize reducing operation cost (runtime). Increasing w_{depth} and w_{mult} shifts the policy toward circuits with lower noise growth, but this often comes at the cost of additional operations, leading to slower execution. We quantify this speed/noise trade-off in Sec. 7.6.

5.3.2 Reward Structure. To guide the agent’s learning process, the reward signal is composed of two parts. The first is an immediate reward provided after every action during training, which guides local, incremental improvements. The second is a terminal reward provided once the entire optimization sequence for a given expression has ended (end of episode), and which guides the agent toward a globally optimal solution.

i) Step Reward (R_{step}): After each action, the agent receives an immediate reward calculated as the relative percentage improvement in the cost function. If the cost of the expression before the action is C_t and after is C_{t+1} , the reward of the step is:

$$R_{\text{step}} = \frac{C_t - C_{t+1}}{C_t}$$

ii) Terminal Reward (R_{final}): The reward is given at the end of an episode (when the agent selects the END action, or the pre-defined maximum steps limit for the episode is reached).

This reward is based on the total percentage reduction in cost from the initial state of the expression (C_{initial}) to its final state (C_{final}):

$$R_{\text{final}} = \left(\frac{C_{\text{initial}} - C_{\text{final}}}{C_{\text{initial}}} \right) \times 100$$

Terminal reward motivation. We initially trained the CHEHAB RL agent using only the step reward and found that the policy often became locally greedy: it favored rewrite sequences that yield small early improvements and avoided transformations that temporarily increase cost but unlock larger gains later. This behavior is expected because PPO optimizes discounted returns, which biases learning toward immediate improvements. To better handle delayed credit in rewrite optimization, we add a terminal reward based solely on the final optimized expression, which encourages sequences that optimize end-to-end circuit quality rather than only short-horizon gains.

We quantify the impact of removing R_{final} (i.e., using only the immediate reward) in Sec. 7.6, showing that the combined *immediate+terminal* reward yields better end-to-end execution time compared to step-only reward.

5.4 Actor-Critic Networks

In this work, we adopt the actor-critic RL architecture. To manage the complexity of the action space, we learn a *hierarchical stochastic policy* (actor), which decomposes the action a into two components: a rewrite rule r and an application location p . This policy is defined by two conditional probability distributions: $\pi_{\theta_1}(r | s)$ for rule selection and $\pi_{\theta_2}(p | s, r)$ for location selection. Alongside the policy, we learn a value function (critic) $V_{\phi}(s)$, which estimates the expected return from a given state s . The policy and critic networks are implemented as separate deep neural networks.

5.4.1 Rule Selection Network. The first network of the actor is the rule selection network. It is a Multi-Layer Perceptron (MLP) that takes, as input, the 256-dimensional state embedding generated by the Transformer encoder (Section 5.1). The network consists of two fully connected hidden layers with 128 and 64 neurons, respectively, each using the ReLU activation function. The network’s final output layer is followed by a softmax, which produces a probability for each available action from the action space. After invalid actions (non-matching rules) are masked, the agent samples from this resulting probability distribution to select its next action.

5.4.2 Location Selection Network. Once the rule network selects a rewriting rule, the Location Network selects the location within the IR for its application. The network selects whether the rule is applied to its 1st match in the IR, 2nd match, 3rd match, etc. It is implemented as an MLP that takes two inputs: the 256-dimensional state embedding and the output from the actor network representing the chosen rule. Its architecture consists of two fully connected hidden

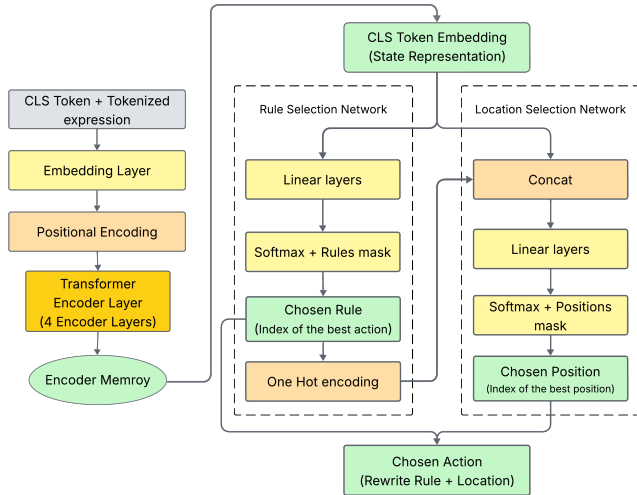


Figure 4. Architecture of the Policy Network

layers, each with 64 neurons, followed by ReLU activation. The final output layer produces a probability distribution over locations, from which the final position is sampled.

5.4.3 The Critic (Value Network). The critic network estimates the value function, $V(s)$, which predicts the expected cumulative future reward from the current state. It is an MLP that takes the state embedding as input. Its architecture consists of 3 fully-connected hidden layers with 256, 128, and 64 neurons, respectively, each with a ReLU. The final layer is a linear output layer that produces a single scalar value representing the value estimate, $V(s)$. This estimate is used during training to assess the actor’s actions and guide the learning.

6 Training Data

A key challenge for training an effective CHEHAB RL agent is the absence of datasets for FHE programs. Consequently, we need to generate a dataset of expressions that are both diverse and contain realistic code patterns that appear in practice.

Limitations of Random Data Generation. Training on purely random expressions is not ideal. Randomly generated expressions do not follow the same distribution of programs encountered in practice. They often lack the specific computational patterns that appear in practice (e.g., common sub-expressions, opportunities for factorization, and structured arithmetic that can be vectorized).

LLM-guided Generation. To address the previous limitation, we use *Large Language Models (LLMs)* to generate the training data. This design choice is important in practice: Sec. 7.6 shows that training on LLM-generated programs yields substantially better policies than training on randomly generated programs. The full prompt template and a link to the generated training dataset are provided in Appendix F. We guide the LLM to synthesize a dataset that is diverse and rich in optimizable code patterns. Since the LLM is trained

on a large corpus of realistic code, it tends to generate code that follows the same distribution of realistic code. For our data generation, we used the *Gemini 2.5 Flash* model. The prompt provided to the LLM is structured to give it sufficient context about the problem domain, and includes:

i) Syntax and Semantics: A formal description and multiple examples of the CHEHAB IR, covering scalar operations, vector constructors (Vec), and vector operations (e.g., VecAdd).

ii) Rewrite Rule Examples: Examples of the rewrite rules from our TRS are included to guide the LLM on the specific patterns we intend to optimize.

iii) Real World Examples: To ground the synthesis process in practical computations, the prompt contains real-world kernels as examples. Examples provided in the prompt include: a) Union Cardinality: Computes the cardinality of the bitwise OR of two 4-bit vectors; b) Squared Difference: Computes the element-wise squared error between two vectors; c) 4x4 Matrix Addition: A common linear algebra kernel that performs element-wise addition between two matrices. The provided examples do not include any of the benchmarks used in the evaluation.

iv) High-Level Goal: A description of the optimization objective and an explicit request for structural diversity in the generated expressions.

Synthesizing CHEHAB IR Directly. We also considered generating CHEHAB DSL programs (embedded in C++) and then lowering them through the compiler to CHEHAB IR. In practice, directly generating CHEHAB IR was more reliable and easier to validate: the IR has a small, closed vocabulary and simple typing constraints, making it easier for the LLM to produce syntactically valid programs. In contrast, generating CHEHAB DSL (which is embedded in C++) requires emitting compilable code (including boilerplate C++ code), and validating each sample requires invoking a C++ toolchain and running DSL-to-IR lowering, which significantly slows the generation loop. Direct IR generation also simplifies deduplication and benchmark exclusion, since we can directly parse and canonicalize each program before adding it to the corpus.

Post Processing. Expressions generated by the LLM are filtered to ensure their validity and uniqueness:

i) Parsing and Validation: Expressions that cannot be parsed by our IR parser (due to syntactic errors) are discarded.

ii) Uniqueness Filtering: To ensure diversity and avoid redundancy, we implement a uniqueness filter based on the canonical representation of expressions. This canonical representation is obtained using our Identifier and Constant Invariant (ICI) tokenization. Generated expressions may be semantically equivalent but use different variable names (e.g., $(\text{Vec} (+ x (* y z)))$ and $(\text{Vec} (+ a (* b c)))$). After ICI tokenization, they become equivalent. A newly generated expression is added to the dataset only if its canonical form was not generated before.

iii) *Exclusion of Benchmarks*: To avoid training the RL agent on programs identical to those found in the benchmark, we remove any generated expression that is identical to one of the benchmarks. This ensures the evaluation measures generalization to unseen programs. To do this, we compute the canonical form of each program in our benchmark suite (Sec. 7) using ICI tokenization. Any expression in the generated dataset that matches a benchmark is removed.

Our approach ensures that the dataset is not only syntactically correct but also semantically relevant and rich in the patterns our agent needs to learn to optimize. We generated 15,855 unique expressions using the LLM and used this dataset to train the RL agent.

Generalizability and benchmark separation. We strictly separate training and evaluation. The LLM-generated training dataset contains 15,855 unique expressions. Each expression is parsed and converted to its ICI canonical form, which normalizes away differences in identifiers and constants and collapses common syntactic variants. We use this canonical form to deduplicate the dataset and to remove any generated expression whose canonical form matches a benchmark expression. This ensures that no benchmark program (or a trivially rewritten variant) appears in the training data, so evaluation reflects generalization to unseen programs.

7 Evaluation

We evaluate our proposed approach in three ways:

Quality of Programs Generated. We compare code generated by CHEHAB RL with that produced by the Coyote [52] compiler. The comparison focuses on the execution time of the generated circuit, the number of homomorphic operations, the depth, the multiplicative depth, and noise (noise accumulated by the benchmark, which we want to minimize). The definition of the noise metric and details about how we measure it are in Appendix H.1. We limit our evaluation to FHE compilers that support unstructured code. Porcupine [23] is excluded as it is not publicly available (we reached out to its authors but could not obtain a copy).

Compilation Efficiency. We report the end-to-end compilation time for CHEHAB RL and Coyote.

Ablation Study. We perform an ablation study to evaluate the following: 1) LLM-generated vs random data; 2) CHEHAB RL vs CHEHAB; 3) ICI vs BPE tokenization; 4) Flat vs hierarchical action space; 5) GRU vs Transformer encoder.

7.1 RL Agent Training

We use the Proximal Policy Optimization (PPO) algorithm to train the agent [64] used by CHEHAB RL. We train it for 2 million timesteps (43 hours), on a single multi-core CPU. More details about the training and the hyperparameters in Appendix G and Table 4.

7.2 Benchmarks

We evaluate CHEHAB RL on three benchmark suites. For each benchmark in the benchmark suites, we vary the input size to evaluate the scalability of the compiler. The larger the input is, the larger the program is, since FHE code is fully unrolled. The three benchmark suites are:

Porcupine Benchmark Suite. This is a set of kernels commonly used in linear algebra, machine learning, and image processing. They were used to evaluate Porcupine [23]. They include image processing filters: Box Blur, the x and y gradients of an image (G_x and G_y), and Robert Cross (*Rob. Cross*). The Porcupine benchmark suite also includes Dot Product, Hamming Distance (*Hamm. Dist.*), L2 Distance, Linear Regression (*Linear Reg.*), and Polynomial Regression (*Poly. Reg.*), which are building blocks for ML applications. We include all of the benchmarks that were used to evaluate Porcupine.

Coyote Benchmark Suite. It includes kernels that were used to evaluate Coyote [52]. These kernels are: 1) matrix multiplication (*Mat. Mul.*); 2) a sorting algorithm (*Sort*) that sorts a list of elements; This sorting algorithm is an unstructured code that implements sorting using a tree (as described by Malik et al. [52]). 3) *Max* kernel. This is an unstructured code that finds the maximum element in a list. Coyote also includes three other kernels, which are the dot product, the L2 distance, and a convolution, but these are common with the Porcupine benchmark suite, and therefore, we do not evaluate them again. All of the benchmarks that were used to evaluate Coyote are included in our benchmark suite.

Randomly Generated Irregular Polynomials. The Coyote compiler also uses a set of randomly generated unstructured polynomials for evaluation. We use the same methodology for evaluation. This set of polynomials is a stress test to further investigate the ability of the compiler to vectorize code in the absence of a regular structure in the code. Several polynomials are generated as random arithmetic expression trees. In these polynomials, a polynomial is named tree-X-Y-Z, where high values for X-Y indicate that the polynomial tree is full, complete, and well-balanced, making it easier to vectorize, while low values for X-Y indicate that the tree is sparse and imbalanced, making it harder to vectorize. Z indicates the depth of the tree of the polynomial. We provide more details about these polynomials in Appendix H.3.

7.3 Input Layout Transformation Before Encryption

Vectorization often requires rearranging the layout of the input data so that operands line up in the same ciphertext slots. If performed after encryption, this layout transformation translates into extra ciphertext rotations (and masking), which are expensive. CHEHAB therefore moves this step to the client: inputs are permuted/packed in plaintext and only then encrypted, so the server-side computation starts from ciphertexts already in the desired layout and avoids the

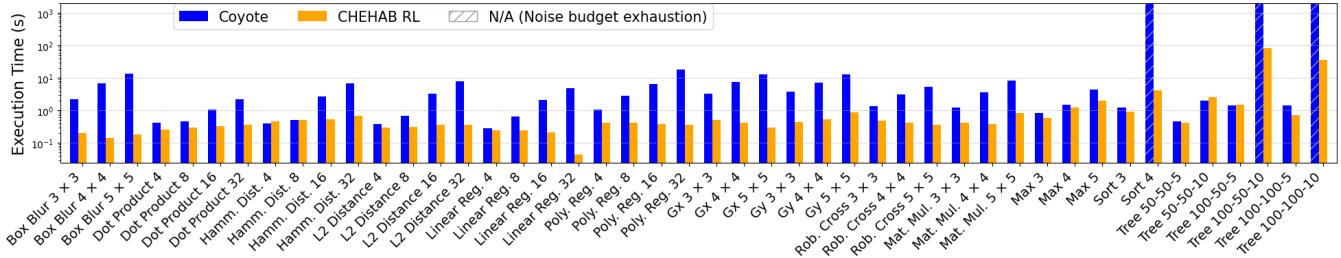


Figure 5. Semi-log plot of execution time of the benchmarks, comparing code generated using our compiler and Coyote.

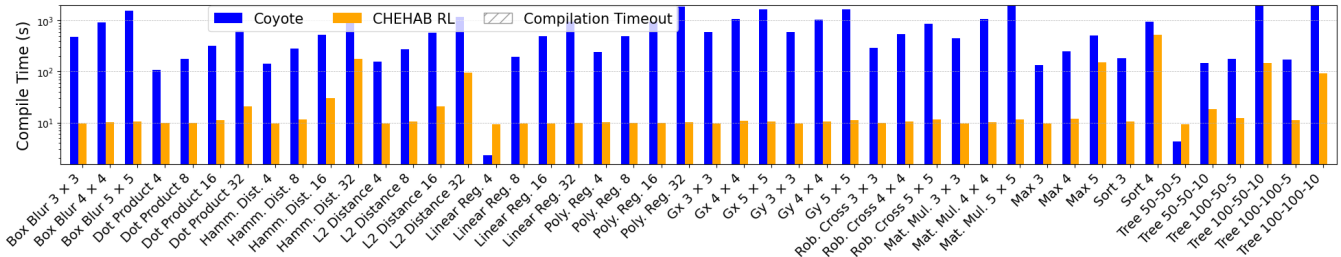


Figure 6. Semi-log plot of compilation time of the benchmarks using our compiler and Coyote.

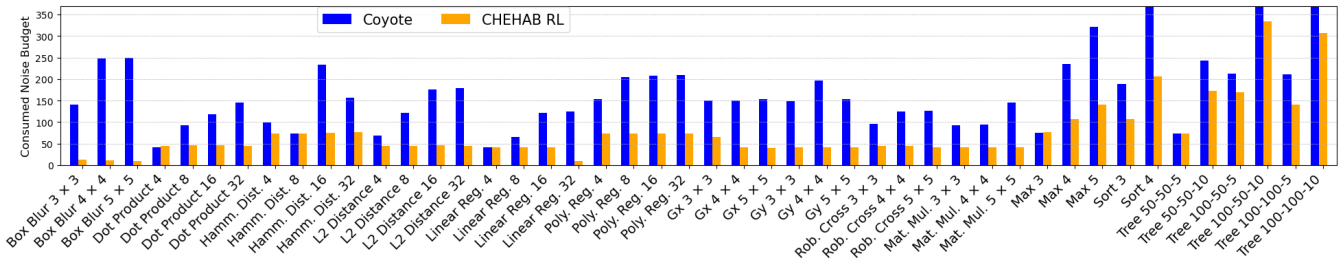


Figure 7. Semi-log plots comparing the Consumed Noise Budget in Coyote and CHEHAB RL.

corresponding homomorphic rotations. Unless stated otherwise, the evaluation reports results with this optimization enabled, and we provide results without this optimization in the appendix.

7.4 Environment Setup

We evaluate our benchmarks on a 2.40 GHz Intel(R) Xeon(R) CPU E5-2680 v4 with 256 GB DDR4 of memory running CentOS Linux 8. The encryption parameters for CHEHAB and Coyote are set as follows: $n = 16384$ (polynomial modulus degree) and q is the default coefficient modulus proposed by the SEAL library for a standard 128-bit security level. We disable the CHEHAB pass for automatic rotation key selection (presented in Appendix B), since Coyote does not have a similar pass. We also disable the use of the blocking technique [52] for both compilers, CHEHAB and Coyote, since both of them perform blocking in the same way. Blocking is a technique that involves vectorizing smaller kernels separately and then composing the resulting vectorized programs. While this technique enables the two compilers to scale to larger programs, our goal is to compare the fundamental algorithms proposed by each compiler on a single block. Since the blocking method is identical in the two compilers, comparing on a single block will better illustrate the

fundamental differences between the two approaches. By default, CHEHAB transforms the data layout of input data before encryption (as described in Sec. 7.3). Results when the data layout of input data is transformed after encryption are presented in the appendix in Table 6. We also use the same SEAL library in both compilers (SEAL version 4.1). We run all the experiments 30 times and report the median execution times and compilation times. The compilation timeout for both compilers was 7200 seconds.

7.5 Evaluation on the Benchmarks

We compare CHEHAB RL with Coyote on our benchmark suite, measuring the execution time of optimized code (Fig. 5), compilation time (Fig. 6), and consumed noise budget (Fig. 7). Fig. 5 shows that CHEHAB RL produces faster code than Coyote for most benchmarks. On average, CHEHAB RL generates code that is $5.3\times$ faster in execution (geometric mean) than Coyote. For example, on `Poly. Reg. 32`, code generated by CHEHAB RL is $50\times$ faster than code generated by Coyote, and faster by $114\times$ on `Linear Reg. 32`. This speedup is due to having fewer operations in code generated by CHEHAB RL, for example, in `Poly. Reg. 32`, CHEHAB RL generated a circuit with just 3 additions and 2 ct-ct multiplications (ciphertext-ciphertext multiplications).

In contrast, Coyote generates a much larger circuit with 12 additions, 2 ct-ct multiplications, 1 subtraction, 173 ct-pt multiplications (ciphertext-plaintext multiplications), and 134 rotations. Coyote appears to generate a complex data layout that requires extensive rotations and ct-pt multiplications to execute, where CHEHAB RL finds a simpler, more direct vectorization. This pattern holds for `Linear Reg. 32` as well, where the agent produces a circuit with 2 additions, 1 ct-ct multiplication, and 1 ct-pt multiplication, while Coyote generates one with 4 additions, 1 ct-ct multiplication, 3 subtractions, 46 ct-pt multiplications, and 44 rotations. Image-processing kernels also show substantial gains: code generated by CHEHAB RL for `Gx 5x5` is 42× faster than Coyote. In this benchmark, Coyote over-rotates data, leading to a higher number of operations and a slower circuit. For `Tree 50-50-10`, Coyote generates a circuit that runs faster; this is due to the high number of expensive ct-ct multiplications that CHEHAB RL generates. The generated circuits that Coyote generates, despite having a higher number of total operations (21 adds, 19 plaintext multiplications, 7 rotations), require only 7 ct-ct multiplications. In contrast, the circuit produced by CHEHAB RL, while more compact (18 adds, 2 rotations), requires 15 ct-ct multiplications.

Fig. 6 shows that despite producing circuits that are faster to execute, the compilation time for CHEHAB RL is also consistently faster than Coyote’s. On average, the CHEHAB RL compilation process is 27.9× faster (geometric mean) than Coyote. A notable exception to this trend is the `Tree 50-50-5` and `Linear Reg. 4` benchmarks, where Coyote’s compilation time is faster than CHEHAB RL. These benchmarks are small, so Coyote’s search algorithm can rapidly explore the small search space. In contrast, our RL agent requires a series of steps to apply its learned policy. The overhead of invoking the neural network for each of these sequential steps results in a longer compilation time for these small benchmarks. However, as demonstrated across the rest of the benchmark suite, this overhead for the RL agent is outweighed by its higher scalability to larger circuits.

Fig. 7 compares the noise budget consumed by the circuits generated by CHEHAB RL and Coyote. The results show that code generated by CHEHAB RL consistently consumes less noise budget compared to Coyote. On average, code generated by CHEHAB RL consumes 2.54× less noise budget (geometric mean) compared to Coyote. For example, code generated by CHEHAB RL for `Poly. Reg. 32` consumes only 73 bits from the available noise budget (which is 369 bits), leaving a remaining budget of 296 bits, while Coyote’s much larger and complex circuit consumes 210 bits. In different benchmarks such as `Sort 4` and two of the `Polynomial Tree` benchmarks, the circuit generated by Coyote exhausts the entire noise budget and fails to execute, while CHEHAB RL successfully produces valid, runnable circuits for all benchmarks, leaving a safe remaining noise budget in each case.

$(w_{\text{ops}}, w_{\text{depth}}, w_{\text{mult}})$	Exec. time (\times vs. (1, 1, 1))	Noise (\times vs. (1, 1, 1))
(1, 50, 50)	1.426×	0.941×
(1, 100, 100)	1.487×	0.935×
(1, 150, 150)	1.396×	0.911×

Table 1. Reward weight sensitivity.

A more detailed comparison, including operation counts for all benchmarks, is available in Table 6 in Appendix I.

7.6 Ablation Study

Step vs. step+terminal reward. Our reward signal is composed of an immediate step reward and a terminal reward (Sec. 5.3.2), where the step reward provides local feedback after each rewrite and the terminal reward provides a global signal at the end of the optimization episode. We ablate this design by training an agent with only the immediate reward (step wise) and comparing it to our default agent using immediate + terminal rewards. Using both components is beneficial: *immediate+terminal* achieves a 1.291× better execution time (geometric mean) than using the immediate reward alone. This shows that the terminal reward is necessary to align the policy with end-to-end circuit quality, whereas purely local feedback can over-emphasize short-horizon improvements that do not translate into the best final circuit. Figure 9 shows the per-benchmark execution time.

Reward weight sensitivity. We further ablate the reward design by varying the weights of the cost function in Sec. 5.3.1, i.e., $(w_{\text{ops}}, w_{\text{depth}}, w_{\text{mult}})$. We compare the default (1, 1, 1) against a set of new weights: (1, 50, 50), (1, 100, 100) and (1, 150, 150). We include configurations with large w_{depth} and w_{mult} because operation costs in C_{ops} are already numerically large, and thus depth-based penalties must be scaled to have a comparable influence when explicitly biasing the policy toward lower-depth circuits. While the new weight variants have a slightly lower noise consumption (they consume 0.911-0.941× the noise of (1, 1, 1)), our default weight configuration, (1, 1, 1), yields significantly better runtime: it is 1.396-1.487× faster in execution time (geometric mean) than the other variants. This is summarized in Table 1.

LLM-generated vs. Random Data. To quantify the effectiveness of using an LLM to generate data, we compare the performance of our RL agent (trained on LLM-generated data) against the same agent trained on a dataset of randomly generated data. The random code generator uses a standard approach to generate code with a uniform distribution (described in Appendix H.2). Fig. 8 compares the two approaches. The agent trained on LLM-generated data produces FHE circuits that are faster. For instance, on the `L2 Distance 32` benchmark, CHEHAB RL trained on LLM-generated data produces code that is 13× faster compared to CHEHAB RL trained on randomly generated data. Similar performance gaps of an order of magnitude are observed

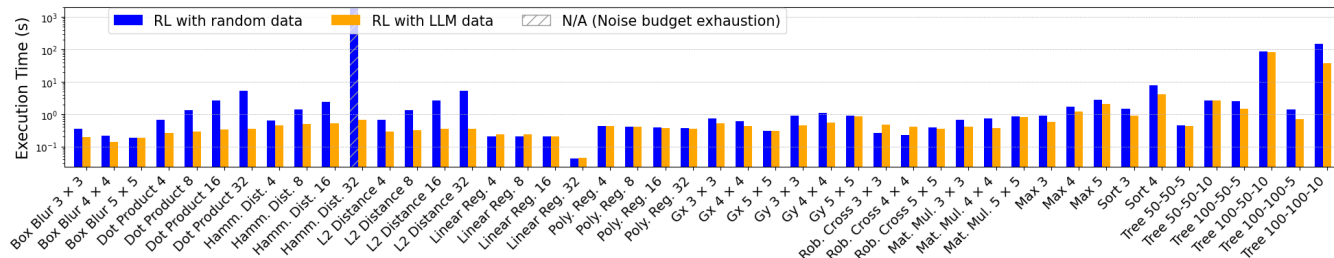


Figure 8. Semi-log plots comparing the execution times when using an RL agent trained with randomly generated data and an RL agent trained with data generated by an LLM

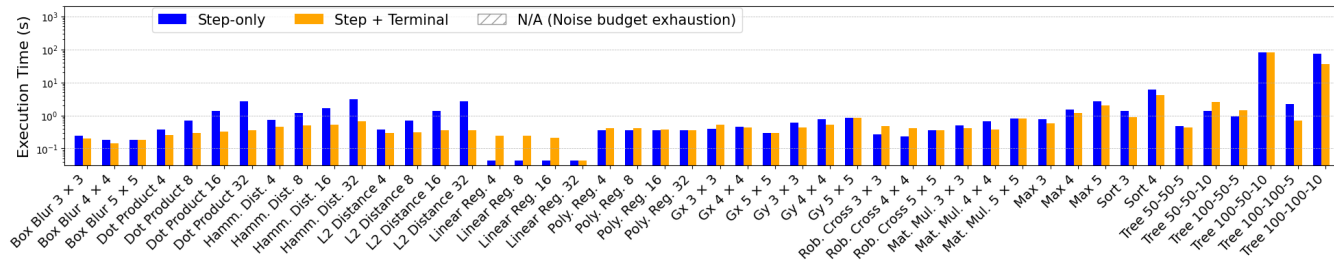


Figure 9. Semi-log plot of benchmark execution time, comparing an agent trained with step-only reward against our step+terminal reward.

across the larger instances of *Hamm. Dist.* and *Dot Product*. This difference in performance is due to the quality of the learned policies. The agent trained on LLM-generated data learns to generate more efficient circuits with fewer expensive homomorphic operations. For example, in the L2 Distance 32 case, the circuit generated by the LLM-trained agent contains only 5 additions and 1 multiplication, compared to 28 additions and 28 multiplications in the circuit generated by the agent trained on random data. This demonstrates that the LLM-generated data helps the RL agent learn a policy that performs better on realistic programs, since it provides expressions with relevant, optimizable structures, that more closely mirror real program distributions.

CHEHAB RL vs CHEHAB. To ensure that the improvements in reducing latency in CHEHAB RL are due to the RL TRS, and not to other optimizations in the original CHEHAB, we compare the execution times of code generated by the original CHEHAB and CHEHAB RL. Fig. 12 (Appendix) shows the results. As we see, in most cases, code generated by CHEHAB RL is faster. In some instances, most notably Gx 3x3, the original CHEHAB is better than CHEHAB RL due to a sub-optimal decision made by the learned policy. An examination of the generated circuit shows that the RL agent chose to apply one rotation to align data for the vectorization of two ct-pt multiplications. While the CHEHAB RL successfully vectorized the operations, the computational cost of the required rotation was greater than the performance benefit gained from vectorizing the two ct-pt multiplications.

ICI vs. BPE Tokenization. We also evaluate the use of the Identifier and Constant Invariant (ICI) tokenization for tokenizing the inputs of the embedding model. This experiment compares our agent, which uses ICI tokenization, against the

same agent that uses a standard Byte-Pair Encoding (BPE) tokenizer. The BPE tokenizer was trained on a corpus of 5 million randomly generated IR expressions to build its vocabulary (details about random IR code generation are in Appendix H.2). Once the BPE tokenizer is trained, we train the two agents using our dataset of LLM-generated data. Fig. 10 in the appendix shows that the RL agent that uses ICI tokenization finishes its 2 million steps training in 43 hours, compared to the RL agent trained with BPE, which takes 68 hours, showing that our tokenization helps accelerate the training.

Flat vs. Hierarchical Action Spaces. We also compared the hierarchical action space against a flat one that enumerates rule-location pairs (i.e. each rule is duplicated multiple times, once for each location). The learning curves in Fig. 13 in the appendix show consistently higher rewards and quicker learning for the hierarchical agent.

GRU vs Transformer. To validate our choice of a Transformer encoder for the state representation, we compared its encoding capabilities against a baseline recurrent architecture, the Gated Recurrent Unit (GRU). Our experiments show that the transformer architecture was able to learn a better representation with less training compute. Details about this experiment are in Appendix I.1.

8 Related Work

This section compares CHEHAB RL and state-of-the-art compilers. Table 2 summarizes the differences, which we discuss in detail in this section. In addition, we discuss the use of RL in compilers, tokenization methods, and random data generation methods in Appendix J.

Table 2. COMPARISON WITH RELATED WORK.

	CHEHAB RL	HECO	Porcupine	Coyote	Ramparts	EVA	HECATE
Feature							
Vec. struct. code	✓	✓	✓	✓	×	×	×
Vec. unstruct. code	✓	×	✓	✓	×	×	×
Reduce mul. depth	✓	✓	✓	×	✓	×	×
Auto datalayout	✓	×	×	✓	✓	✓	✓
Data driven	✓	×	×	×	×	×	×
Scheme	BFV	BFV CKKS BGV	BFV	BFV	BFV	CKKS	CKKS

FHE Compilers for Automatic Vectorization. Recent work [23, 27, 52, 72] focuses on the problem of transforming FHE programs that use scalar variables into vectorized programs (batching). Our work is similar to these compilers since it also takes a scalar code and vectorizes it. Unlike HECO [72], CHET [27], ANT-ACE [50], Orion [30], HEIR [4] and Qiwu [75] which only support the vectorization of structured (loop-based) code, CHEHAB RL is designed to support both structured and unstructured code. Compared to Coyote [52], our approach scales better. Unlike Porcupine, in which the user has to manually provide the data layout of the vectorized code, our approach computes the best data layout automatically.

FHE Compilers for Circuit Optimization. These compilers do not vectorize their input code. They focus on applying other optimizations (other than vectorization). These compilers include EVA [26], Ramparts [5] and HECATE [49]. The main challenges that they target are automatic parameter selection, the scheduling of ciphertext-maintenance operations, reducing the multiplicative depth of circuits, and reducing the number of operations in a circuit. Our approach is complementary to the above compilers. First, it supports code vectorization, and therefore, code vectorized by our approach can be passed to these compilers for further optimization. Our approach also offers the ability to reduce the depth of circuits, which they do not address. Appendix J provides a more detailed comparison with these compilers.

General Purpose Vectorization in non-FHE Programs. Superword-Level Parallelism is a classical technique used for code vectorization [47]. It processes a sequence of scalar instructions to create vector packs or groups of isomorphic instructions that can be packed together into vectors. Since it does not depend on the presence of data-parallel loops in the code, it is well-suited for vectorizing unstructured code. However, while creating vector packs, SLP does not consider the high cost of rotations in FHE programs, which results in code that has a high number of rotations, making it impractical for the domain of FHE, where rotations are expensive. goSLP [53] is a state-of-the-art SLP approach that formulates the vectorization problem as an Integer Linear Programming (ILP) problem. However, it operates at a level

closely tied to the target architecture, where the vectors are restricted to a maximum width of four elements. One of its key limitations is that while it efficiently handles the pairwise packing of statements, extending this to pack more than two statements makes the problem intractable for current solvers. In contrast, our approach for FHE supports significantly larger vectors (in the thousands), which is necessary for the domain of FHE since vectors in FHE are significantly larger. VeGen [19] extends SLP by introducing lane-level parallelism, tracking how individual lanes execute computations. This enables VeGen to account for rotation costs when constructing vector packs. However, this reasoning is local, as VeGen does not consider the impact of instruction packing on subsequent rotations. Other work [31, 60, 63] also addresses code vectorization but is not designed for the field of FHE and does not assume a high cost for rotations. In addition, in this work, our goal is to develop an FHE compiler that not only vectorizes code but also reduces the instruction latency and noise growth while being more scalable.

RL for Code Optimization. RL has been explored for compiler code optimization [10, 16, 25, 36, 59, 69, 71, 74]. Systems such as *Halide RL* [59] train agents to select schedules for image processing code, while *Tiramisu RL* [10] applies polyhedral transformations to computational kernels using an RL-based policy. More specialized approaches include *NeuroVectorizer* [36], which learns to select the optimal vectorization and interleaving factors for loops on SIMD architectures using learned code embeddings, and *Polygym* [16], which frames affine loop transformation in the polyhedral model as a Markov Decision Process. Frameworks such as *CompilerGym* [25] have provided RL environments for tasks such as LLVM phase ordering. While previous work addresses traditional code optimizations, it does not consider the unique constraints of Fully Homomorphic Encryption. Our work is the first to formulate FHE optimization as an RL problem, where the agent must learn a policy that navigates the trade-offs between vectorization, cryptographic noise accumulation, and the cost of operations. Appendix J provides more details on using RL for code optimization.

Automatic Code Optimization in Compilers. Automatic code optimization for loop nests has been widely explored. Examples of state-of-the-art methods include the use of the polyhedral model and deep-learning-based methods [7, 8, 11, 13, 18, 34, 38, 42, 54, 67, 76]. Such work does not address FHE code optimization, though.

9 Conclusion

This paper introduces a novel framework that leverages RL to automate FHE code optimization. Our proposed approach trains an RL agent to learn a policy for applying a sequence of rewriting rules to automatically vectorize scalar FHE code while reducing instruction latency and noise growth. We

show that our approach generates code that is $5.3\times$ faster than Coyote, accumulates $2.54\times$ less noise, while it takes $27.9\times$ less time in compiling code, enabling better scalability.

Acknowledgment

This research was partly supported by the Center for Cyber Security (CCS) at New York University Abu Dhabi. It was also partly supported by the Center for Artificial Intelligence and Robotics (CAIR) at New York University Abu Dhabi, funded by Tamkeen under the NYUAD Research Institute Award CG010. It was also partly supported by the Federation of Arab Scientific Research Council under contract number ARICA23_787. The research was carried out on the High-Performance Computing resources at New York University Abu Dhabi.

A More Detailed Background

A.1 Term Rewriting System (TRS)

A term rewriting system (TRS) is a set of rewrite rules that transform an expression to a new form (rewrite it into a new expression). Let us take a simple example of a TRS system to illustrate how it works. Let us assume that we want to simplify arithmetic expressions and let us assume that we have the following rule set $S = \{t - t \rightarrow 0, t + 0 \rightarrow t\}$. Let us use this rule set S to rewrite and simplify the expression $b + (a - a)$. The rule $t - t \rightarrow 0$ can be applied to simplify the expression $a - a$. After applying the rule, we get the new expression: $b + 0$. Now we can apply the rule $t + 0 \rightarrow t$ to simplify the previous expression into b .

A.2 Fully Homomorphic Encryption

Fully Homomorphic Encryption (FHE) enables computations directly on encrypted data [6, 20]. A *homomorphism* is a function between two groups that preserves their structure [29]. In the context of FHE, these groups correspond to elements in the plaintext space \mathcal{P} and the ciphertext space \mathcal{C} . Let us define the encryption and decryption functions as $E(\cdot) : \mathcal{P} \mapsto \mathcal{C}$ and $D(\cdot) : \mathcal{C} \mapsto \mathcal{P}$, respectively. Given an operation \circ on plaintexts and its homomorphic counterpart \odot on ciphertexts, for plaintexts $m_a, m_b \in \mathcal{P}$ with encryptions $c_a = E(m_a), c_b = E(m_b) \in \mathcal{C}$, the homomorphic property ensures that operations on encrypted data remain consistent with their plaintext counterparts, i.e., $m_a \circ m_b = D(c_a \odot c_b)$.

A.2.1 BFV Scheme. The BFV encryption scheme [32] is an FHE scheme based on the Ring-Learning With Errors (RLWE) problem [51]. In BFV, the plaintext space is defined as $\mathcal{P} = R_t = \mathbb{Z}_t[x]/(x^n + 1)$, while the ciphertext space is $\mathcal{C} = R_q \times R_q$, where $R_q = \mathbb{Z}_q[x]/(x^n + 1)$. Here, n is the polynomial modulus degree, and t, q , and $x^n + 1$ denote the plaintext, ciphertext, and polynomial moduli. Typical values for t range from 16 to 32 bits, while q varies between 100 and 900 bits. The degree n is usually a power of two, commonly between 2^{10} and 2^{16} , as recommended by the *Homomorphic Encryption Standard* [3].

A.2.2 FHE Batching. Batching enables evaluation of a function on n blocks of data [15] at once by encoding a vector of n messages in a single plaintext polynomial in R_t . Under the assumption $t \equiv 1 \pmod{2n}$, $x^n + 1$ factors into linear polynomials modulo t , i.e. $x^n + 1 \equiv \prod_{i=1}^n (x - a_i) \pmod{t}$, with $a_i = a^{2^{i-1}}$ being the $2n^{\text{th}}$ primitive root of unity modulo t , and $t = \prod_{i=1}^n t_i$ where t_i are prime ideals with basis $(t, x - a_i)$. Using CRT on ideals, we have the following isomorphism:

$$R_t = R/(t) \stackrel{CRT}{\cong} R/t_1 \times \cdots \times R/t_n$$

Thus, evaluating a function once over $R/(t)$ evaluates the same function on smaller plaintext spaces $R/t_1, \dots, R/t_n$.

B Selection of Rotation Keys

B.1 Importance of Selecting the Rotation Keys

Galois keys (a.k.a. rotation keys) are essential for performing rotation operations in FHE. Each distinct rotation step requires its own key—for example, rotating a ciphertext by s_1 and another by s_2 (where $s_1 \neq s_2$) necessitates two separate rotation keys. When a program involves many unique rotation steps, generating and transmitting all keys becomes costly, as each key is several megabytes in size. A common approach to mitigate this is to generate a subset of rotation keys and express other rotations as combinations of these. For instance, generating only the rotation key for step $s = 1$ allows any rotation to be performed as repeated single-step rotations. This reduces key generation and communication costs but significantly increases execution time and noise for large rotation steps. A better trade-off is to balance the costs of key generation and communication, as well as the cost of executing rotations during homomorphic operations.

B.2 Method for Selecting Rotation Keys

After code optimizations, CHEHAB generates an IR containing the necessary rotations for which keys must be generated. Previous work [5, 23, 49, 72] does not address automatic rotation key selection, relying instead on the FHE library’s default, which generates $2 \log_2(n)$ keys. This approach can be suboptimal, as some applications may require fewer than $2 \log_2(n)$ rotation keys. Instead, CHEHAB selects the rotation keys to be generated and ensures that the number of keys does not exceed a user-defined upper bound β , which defaults to $2 \log_2(n)$.

Let χ be the set of all rotation steps used in the program. Our goal is to decompose the steps in χ . We use the non-adjacent form (NAF) representation of each step s in χ to decompose it. For example, possible decompositions of a step $s = 3$ are obtained by calculating $NAF(3)$. The NAF representation writes s as a sum of powers of two, where each coefficient is either $+1$ or -1 , and no two nonzero digits are adjacent. For example, $NAF(3) = 4 - 1$; $NAF(5) = 4 + 1$.

Once we calculate the NAF representation for each step s , we collect the decompositions of the steps. For each rotation step s , let Γ_s denote the set of decompositions of s obtained from its NAF (e.g., for $s = 3$ we get $\Gamma_3 = \{-1, 4\}$).

We then select a subset Ω of the rotation steps in χ that will be decomposed via their NAF. The remaining rotation steps that are not decomposed form another set, denoted χ_f .

The final set of rotation keys to be generated is the union of the keys for the non-decomposed rotations and those derived from the NAF decompositions.

Consider the following example:

$$\begin{aligned} \chi &= \{1, 2, 3, 4, 5, 6, 7, 9, 10, 12, 11, 13, 15\} \\ n &= 16, \quad 2 \times \log_2(n) = 8, \quad \beta = 9 \end{aligned}$$

The NAF decompositions of steps in χ are as follows:

$$\begin{aligned}
NAF(1) &= 1, & NAF(2) &= 2, & NAF(3) &= -1 + 4 \\
NAF(4) &= 4, & NAF(5) &= 1 + 4, & NAF(6) &= -2 + 8 \\
NAF(7) &= -1 + 8, & NAF(9) &= 1 + 8, & NAF(10) &= 2 + 8 \\
NAF(12) &= -4 + 16, & NAF(11) &= -1 - 4 + 16 \\
NAF(13) &= 1 - 4 + 16, & NAF(15) &= -1 + 16 \\
\Gamma_1 &= \{1\}, & \Gamma_2 &= \{2\}, & \Gamma_3 &= \{-1, 4\} \\
\Gamma_4 &= \{4\}, & \Gamma_5 &= \{1, 4\}, & \Gamma_6 &= \{-2, 8\} \\
\Gamma_7 &= \{-1, 8\}, & \Gamma_9 &= \{1, 8\}, & \Gamma_{10} &= \{2, 8\} \\
\Gamma_{12} &= \{-4\}, & \Gamma_{11} &= \{-1, -4\} \\
\Gamma_{13} &= \{1, -4\}, & \Gamma_{15} &= \{-1\}
\end{aligned}$$

A valid set of rotation steps selected for decomposition is:

$$\Omega = \{1, 2, 3, 4, 5, 6, 7, 9, 12, 15\}$$

In that case, the final state is:

$$\begin{aligned}
\chi_f &= \{10, 11, 13\} \\
\Gamma_{tot} &= \bigcup_{s \in \Omega} \Gamma_s = \{1, 2, 4, -1, -4, 8\}
\end{aligned}$$

where Γ_{tot} is the set of decompositions of steps in χ selected for decomposition. At the end, we end up with a smaller number of rotation keys to generate, since we just need to generate 9 keys (a key for each step in $\chi_f \cup \Gamma_{tot}$), instead of generating 13 keys (a key for each rotation step in χ).

C CHEHAB DSL syntax and semantics.

CHEHAB is an *embedded* DSL implemented via C++ operator overloading on Ciphertext and Plaintext. Although CHEHAB programs are written in C++, only a restricted subset of C++ expressions and helper functions constitutes the DSL. We therefore summarize this *practical DSL subset* as a compact grammar for readability, while keeping the full operator list in Table 3 as a reference.

C.1 Core expression grammar (pseudo-grammar).

Programs in CHEHAB construct expression graphs over Ciphertext or Plaintext values:

$$\begin{aligned}
e ::= & x \mid k \mid (e) \mid e \oplus e \mid -e \mid e \rho \mid k \\
& \mid f(e) \mid g(\{e_1, \dots, e_n\}) \mid e.set_output("name")
\end{aligned}$$

where x is an identifier, k is an integer literal, $\oplus \in \{+, -, *\}$, and $\rho \in \{\ll, \gg\}$.

The supported helper functions are:

$$\begin{aligned}
f \in & \{\text{square}, \text{reduce_add}, \text{reduce_mul}, \text{SumVec}, \text{encrypt}\}, \\
g \in & \{\text{add_many}, \text{mul_many}\}.
\end{aligned}$$

Pseudo-semantics. Expressions are typed as Ciphertext or as Plaintext. Binary operators denote the corresponding homomorphic operations (ct-ct or ct-pt variants depending on operand types), unary $-$ denotes negation, and \ll/\gg denote slot rotations by a constant offset. Helper functions expand into compositions of these primitives (e.g., square

and exponentiate as repeated multiplication, add_many and mul_many as reductions over a set of expressions, while reduce_add, reduce_mul and SumVec as structured reductions). Integer literals are permitted in expressions via implicit Plaintext construction (and encrypt when needed). Finally, set_output("name") marks an expression as a program output for compilation.

C.2 List of Operations in the CHEHAB DSL

Table 3 provides the full list of operations in the CHEHAB DSL as well as their signatures and descriptions.

Table 3. Operations of the CHEHAB domain-specific language (ct: ciphertext, pt: plaintext, int: integer).

Op.	Signature	Description
+	ct × ct → ct ct × pt → ct pt × ct → ct	Element-wise addition
+	ct × int → ct	Add int value to all elements of ct
-	ct × ct → ct ct × pt → ct pt × ct → ct	Element-wise subtraction
-	ct × int → ct	Subtract int value from all elements of ct
-	ct → ct	Negation of each element of the argument
<<	ct × int → ct	Rotation of ciphertext to the left with the given step
>>	ct × int → ct	Rotation of the ciphertext to the right with the given step
*	ct × ct → ct ct × pt → ct pt × ct → ct	Element-wise multiplication
*	ct × int → ct	Multiply all ciphertext elements by an int

D Code Generation

To reduce memory consumption, CHEHAB minimizes the creation of temporary ciphertext and plaintext objects using the primitive *inplace* provided by the SEAL API. This primitive enforces the reuse of memory occupied by dead objects, similar to how a compound assignment operator works. To compile a program, the user runs the DSL code. When the DSL code is run, it creates the IR AST, runs the compiler passes on the IR, and generates optimized code at the end (C++ code). This code is further compiled using a C++ compiler. The generated binary code is the final outcome of the compilation process and can be run like any other binary. This approach is common in implementing DSLs embedded in C++.

E Rewriting Rules

The transformations available to the RL agent are defined as a set of rewriting rules. These rules include rules for vectorization, algebraic simplification, and rotation.

Vectorization Rules for Isomorphic Subexpressions.

These rules pack scalar arithmetic operations into single vector instructions. They search for isomorphic element-wise scalar expressions and rewrite them as a single vector instruction. For example, a vectorization rule for addition is:

$$(\text{Vec } (+ a b) (+ c d)) \Rightarrow (\text{VecAdd } (\text{Vec } a c) (\text{Vec } b d))$$

This rewriting rule replaces two scalar additions (left-hand side) with one vector addition operating on newly constructed vectors of the operands (right-hand side). Similar rules exist for multiplication, subtraction, and negation.

Vectorization Rules for Non-isomorphic Subexpressions. While powerful, the previous vectorization rules require isomorphic subexpressions. To handle common patterns of non-isomorphic subexpressions, our set of rules also includes general rules for vectorizing such non-isomorphic patterns. For each arithmetic operation op , we have a rule that matches whenever an expression contains a mix of operations (non-isomorphic subexpressions), provided that the operation op appears more than once. The rule then vectorizes all instances of the operation op . It also moves any non-matching sub-expression (containing operators other than op) into the first operand vector. It then pads the second operand vector with the appropriate identity element (e.g., 1 for multiplication, 0 for addition). For example:

$$(\text{Vec } (* a b) (* c d) (- f g)) \Rightarrow (\text{VecMul } (\text{Vec } a c (- f g)) (\text{Vec } b d 1))$$

Here, the non-isomorphic vectorization rule for multiplication matches because there are two $*$ operations. It packs the two multiplications into a single vector multiplication operation, and leaves $(- f g)$ in the 1st operand, and pads the second operand vector with 1, the multiplicative identity.

Since the RL agent is trained to predict rewriting rules that maximize the global reward, it automatically weights the cost and benefit of applying this type of vectorization and selects this class of rules only if they are beneficial.

Simplification and Algebraic Rules: This category includes standard algebraic rules that simplify expressions, reduce computational complexity, or transform expressions into a different form (that will be useful in later simplifications). These rules aim to lower the circuit’s depth and minimize the number of operations. Examples include:

- **Arithmetic Simplification:** These rules simplify arithmetic expressions, replacing complex or multiple operations with simpler, equivalent ones. Examples of these rules include factorization

$$(+ (* x y) (* x z)) \Rightarrow (* x (+ y z)),$$

identity elimination

$$(x * 1) \Rightarrow x,$$

absorption rules

$$(x * 0) \Rightarrow 0,$$

plaintext consolidation

$$(* (pt a) (* (pt b) x)) \Rightarrow (* (pt (a*b)) x),$$

where a and b are plaintexts.

- **Arithmetic Transformations:** These rules transform arithmetic expressions in a way that enables their simplification later. Examples include commutativity, associativity, and distribution rules.
- **Circuit Balancing:** These rules balance expression trees, reducing their depth (and noise accumulation). For example, a left-leaning tree of multiplications can be balanced to reduce the multiplicative depth:

$$(\text{VecMul } x (\text{VecMul } y (\text{VecMul } z t))) \Rightarrow (\text{VecMul } (\text{VecMul } x y) (\text{VecMul } z t))$$

Rotation Rules: Data alignment is critical in FHE, and rotations are the primary mechanism for moving data within a packed ciphertext. A naive approach to vectorizing unstructured code would require the RL agent to discover a long and potentially inefficient sequence of low-level rotation, masking, and arithmetic operations to correctly align data. To address this, our set includes rules that transform high-level computational patterns directly into efficient, *composite dataflow structures*. These rules encapsulate what would otherwise be multiple low-level steps into a single, high-level transformation. For example, we consider this expression:

$$(\text{Vec } ((+ (* a b) (* c d)) (+ (* e f) (* g h))))$$

A standard vectorization strategy, without leveraging rotations, would result in the following structure:

$$(\text{VecAdd } (\text{VecMul } (\text{Vec } a e) (\text{Vec } b f)) (\text{VecMul } (\text{Vec } c g) (\text{Vec } d h)))$$

This optimized expression requires two vector multiplication operations and one vector addition operation. However, a more sophisticated strategy, enabled by our rotation-based rules, can find a more efficient solution:

$$(\text{VecAdd } V (<< V 2))$$

where $V: (\text{VecMul } (\text{Vec } a c e g) (\text{Vec } b d f h))$

The final result can then be computed by adding this vector V to a rotated version of itself, which effectively sums the required pairs of products into the first two slots. This alternative strategy requires only one vector multiplication operation, one vector addition, and one rotation. Since a vector rotation is cheaper than a vector multiplication in FHE, this second approach is better. By including such composite transformation rules, they help the RL agent to discover these globally optimal strategies that a simpler vectorizer would miss.

E.1 How did we design our rewriting rules?

To construct the rules for the TRS, we began by collecting the rules from Halide’s TRS [58, 62]. Halide is an industrial compiler used for the optimization of image processing and deep learning pipelines. Halide’s expression space includes operations that are not natively supported by fully homomorphic encryption (FHE), such as comparison, division, and modulo operations. Additionally, performance considerations and optimization goals in Halide differ from ours,

as it operates on plaintext data. Therefore, we selected only the rules that are compatible with FHE. Next, we expanded this initial ruleset manually and developed new rules aimed at reducing the number of operations, rotations, depth, and multiplicative depth in FHE programs.

F LLM Prompt Template for CHEHAB IR Synthesis

The full prompt template used to synthesize CHEHAB IR expressions is presented below. The template encodes (i) CHEHAB IR syntax and validity checks, (ii) explicit constraints on vector width and expression depth, (iii) a structural-diversity requirement beyond alpha-renaming, and (iv) worked examples and rewrite-rule context to bias generation toward expressions that benefit from rewrite-based optimization.

Synthesis Prompt

```
[SYSTEM ROLE]
You are a rigorous validator for CHEHAB IR expressions. First
ANALYZE then GENERATE. Enforce structural uniqueness beyond
variable renaming.

[GENERATION PROTOCOL]
##### CHEHAB IR Generation Protocol #####

You will output 5 structurally unique (Vec ...) expressions
for RL training.
Every expression must honour all rules below. If any check
fails, discard the draft and regenerate before replying.

1. Core Vector Form
-----
- Start with (Vec` and contain exactly {vec_size}
sub-expressions**.
Skeleton -> (Vec expr0 expr1 ... expr_n).
- No nested (Vec ...) inside a sub-expression.
- Sub-expression depth: **4 <= depth <= 20**.

2. Syntax / Operator Rules
-----
- Balanced parentheses.
- Operators: + and * are strictly binary; - may be unary or
binary.
- Variables match [a-z][0-9]*[0-9]* (e.g. in_1_0).
- No numeric literal 0 anywhere.
- No degenerate single-term parentheses such as (x).

3. Semantic / Structural Rules
-----
- Structural uniqueness after canonicalising w.r.t.
history/examples.
- Operation asymmetry: avoid identical operator trees across
siblings.
- Expressions must not be trivially vectorisable; a sequence of
rewrite rules
(see Sec 7) should improve depth or multiplicative depth.

4. Mandatory Generation Checklist
-----
1. Draft 5 candidate (Vec ...) lines.
2. Count elements == {vec_size}.
3. Validate parentheses & operator set.
4. Compute depths & variable counts.
5. Canonicalise and check for structural duplicates.
6. Output the clean expressions--one per line, no commentary.
7. At least 3 expressions must have depth > 10.

5. Worked Example Breakdown (Real World Motifs)
-----
Below are full CHEHAB IR programs illustrating real computations.
*Do NOT copy or trivially rename them.*
```

```
- Union-Cardinality (size 1):
(Vec (+ (+ (+ (- (+ v1_0 v2_0) (* v1_0 v2_0)) ... )))

- Squared Difference (size 4):
(Vec (* (- v1_0 v2_0) (- v1_0 v2_0)) ... )

6. Rewrite Rules Context
-----
[The LLM is provided with the following rules to bias generation
toward
optimizable patterns:]
Rewrite { name: "add-vectorize-2", searcher: (Vec (+ ?a0 ?b0) (+
?a1 ?b1)), applicer: (VecAdd (Vec ?a0 ?a1) (Vec ?b0 ?b1)) }
Rewrite { name: "mul-vectorize-4", searcher: (Vec (* ?a0 ?b0) (*
?a1 ?b1)), ... }
Rewrite { name: "comm-factor-1", searcher: (+ (* ?a ?b) (* ?a ?c)),
applicer: (* ?a (+ ?b ?c)) }

... [84 total rules provided] ...

7. Final Output
-----
- Produce exactly 5 valid, structurally distinct (Vec ...)
expressions.
- At least 3 of the generate expressions Must have a depth > 6**.
- The Generated expressions where they match vectorization rules ,
or rules that enables vectorization.
- The Generated expressions must match real world computations and
programs or similar not fully random computations**.
- One expression per line, raw text-no numbering, comments, or
styling.
- Range them from moderately simple to deeply nested.
- If any candidate breaks §§1-3, discard & regenerate before
responding.""
```

Prompt refinement. We refined the prompt iteratively by manually reviewing generated programs and adding constraints to reduce invalid outputs and duplicates. Using this protocol, we generated a training dataset of 15,855 unique expressions, which is available at: https://raw.githubusercontent.com/Modern-Compilers-Lab/CHEHAB/refs/heads/main/RL/fhe_rl/datasets/final_llm_dataset.txt.

G Training Details

The agent was trained on the LLM-generated dataset. We used a single node with a 2.40 GHz Intel(R) Xeon(R) CPU E5-2680 v4 (14 cores) and 256 GB DDR4 of memory running CentOS Linux 8 for the training. We used the *Stable-Baselines3 library* [61] to implement our RL training. To accelerate the collection of experience, we leverage parallel environments. We run multiple independent instances of the optimization environment in parallel (8 in our case), allowing the agent to collect a diverse batch of trajectories simultaneously. To implement this, we leverage multi-processing where each environment runs in its own process, and multiple episodes are collected in parallel across processes. This speeds up the training process.

Each training episode corresponds to the optimization of a single expression and is limited to a maximum length of 75 steps. We found this limit to be sufficient, as the optimization sequences for the majority of expressions in our training and evaluation sets finished well before reaching 75 steps. The

agent was trained for a total of 2 million timesteps, and the training took 43 hours.

Table 4. PPO Hyperparameters for Training.

Hyperparameter	Value
Learning Rate	1×10^{-4}
Discount Factor (γ)	0.99
GAE Lambda (λ)	0.95
PPO Clip Range (ϵ)	0.2
Update Epochs	20
Steps per Update	2048
Batch Size	256
Number of Environments	8

H More Details about the Evaluation

H.1 Noise Measurement

A freshly encrypted ciphertext begins with a large noise budget, and each homomorphic operation consumes a part of it. When the budget reaches zero, decryption fails. Our goal is to minimize the noise budget consumed by code.

To measure the noise budget consumed in each benchmark, we use the `Decryptor::invariant_noise_budget` function provided by the Microsoft SEAL library. In the BFV scheme, every ciphertext carries an error term (noise) that grows as homomorphic operations are performed. SEAL reports the remaining noise budget (in bits).

In our setup, using a polynomial modulus degree of 16384, a freshly encrypted ciphertext has an initial noise budget of 369 bits. After running each benchmark, we query the remaining noise budget and measure the difference from the initial value. The difference is the consumed noise that we report (in bits).

We use a 20-bit plaintext modulus and select the coefficient modulus using SEAL’s helper

```
CoeffModulus::BFVDefault(poly_modulus_degree)
```

This returns a coefficient modulus with a total size of 389 bits (`total_coeff_modulus_bits = 389`), which is consistent with a theoretical maximum initial noise budget of $389 - 20 = 369$ bits (i.e., `total_coeff_modulus_bits - plain_modulus_bits`).

H.2 Random Code Generation

Our random code generator recursively constructs IR expressions. We control this construction by two parameters: maximum depth and vector size. The generator builds expressions by sampling a mixture of scalar operations, vector operations, rotations, and vector constructors. Sampling is balanced across all combinations of depth (1–15) and vector size (1–32), so the model encounters a wide range of shapes and packing patterns.

Concretely, the generator works as follows:

1. It samples a target vector size n and a depth budget d .
2. Starting from a root, it grows an expression tree until the tree depth budget is reached.

Table 5. Notation.

Symbol	Description
\cup	depth including all operations
\cup^{\otimes}	multiplicative depth
\oplus	# of ciphertext additions
\otimes	# of ciphertext-ciphertext multiplications
\odot	# of ciphertext-plaintext multiplications
\boxtimes	# of ciphertext squares
\cup	# of rotations

3. At each node, it picks an operator from $\{\text{scalar op, vector op, Vec constructor}\}$ that is type-compatible and respects the chosen vector size n .
4. Leaves are instantiated with variables or integer constants.
5. The resulting expression is parsed and type-checked into the compiler IR; invalid samples are discarded.

H.3 Randomly Generated Unstructured Kernels

We borrow the following description of the randomly generated irregular polynomials from the original Coyote [52] paper, which proposed the benchmark. Several polynomials are randomly generated to evaluate as arbitrary arithmetic expression trees. The trees are generated according to three different regimes to cover different kinds of programs:

- Dense, homogeneous: The expression tree is both full and complete, and all the operations are isomorphic. In principle, this represents a best case for vectorization. We refer to these as tree-100-100.
- Dense, nonhomogeneous: The expression tree is both full and complete, each operation has a 50/50 chance of being an add or a multiply. Hence, while the trees are structurally similar, the heterogeneity of operations means that vectorization opportunities are restricted. We refer to these as tree-100-50.
- Sparse: Many operations have one leaf node input; the tree is not very balanced. In principle, this represents a worst case for vectorization, where Coyote must work hard to find vectorizable computation. We refer to these as tree-00-50.

The last number in the names of the polynomials indicates the depth of the tree. For example, tree-100-100-5 indicates a dense, homogeneous tree with a depth equal to 5.

I Benchmark Evaluation Results

Table 6 presents several metrics regarding the depth and number of operations for three cases: 1) the initial (naive) implementation of the benchmarks 2) CHEHAB RL’s generated code for each one of the benchmarks, and 3) Coyote’s generated code. The table compares the three cases in terms of circuit depth (\cup), multiplicative depth (\cup^{\otimes}), number of ciphertext-ciphertext multiplications (\otimes), number of rotations (\cup), number of ciphertext-plaintext multiplications (\odot), and number of ciphertext additions (\oplus). We also report CHEHAB’s and Coyote’s compilation times CT (s) and their Consumed Noise budget (CN), where lower values are better.

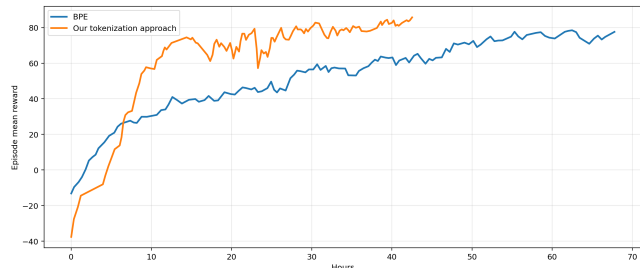


Figure 10. Graph comparing Episode Mean Reward Over Training Time of the CHEHAB RL with ICI tokenization and CHEHAB RL with BPE (both trained for 2 million steps).

The notation used in Table 6 is presented in Table 5. The most important columns in the table are the multiplicative depth (\cup^\otimes), the number of rotations (\cup), the compilation time (CT) for the two compilers, and the Consumed Noise budget (CN). We highlight them in bold.

I.1 GRU vs. Transformer Encoder

To validate our choice of a Transformer encoder for the state representation, we conducted an experiment to compare its encoding capabilities against a baseline recurrent architecture, the Gated Recurrent Unit (GRU). For this comparison, we constructed complete autoencoders for both architectures. The quality of the reconstruction serves as a direct measure of the quality of embedding learned by the encoder; a perfect reconstruction implies that the encoder has preserved all necessary structural information of the program IR. Our RL agent uses only the encoder component, but this autoencoder setup allows us to empirically verify its ability to learn an embedding for the input program.

Experimental Setup. Both autoencoders were trained on the same dataset of 1.4 million randomly generated IR expressions. We use the same methodology described in Sec. H.2 to generate this dataset. The GRU baseline used a 4-layer bidirectional encoder and a 4-layer decoder. The Transformer autoencoder also used 4 encoder and 4 decoder layers, with both models using identical optimizer settings and batch sizes.

Results. The training curves in Fig. 11 and the final test results in Table 7 show a clear distinction in performance. The Transformer autoencoder not only learns significantly faster but also achieves 100% exact-match reconstruction accuracy on the test set. The GRU model, however, plateaus at 98.92% exact-match accuracy.

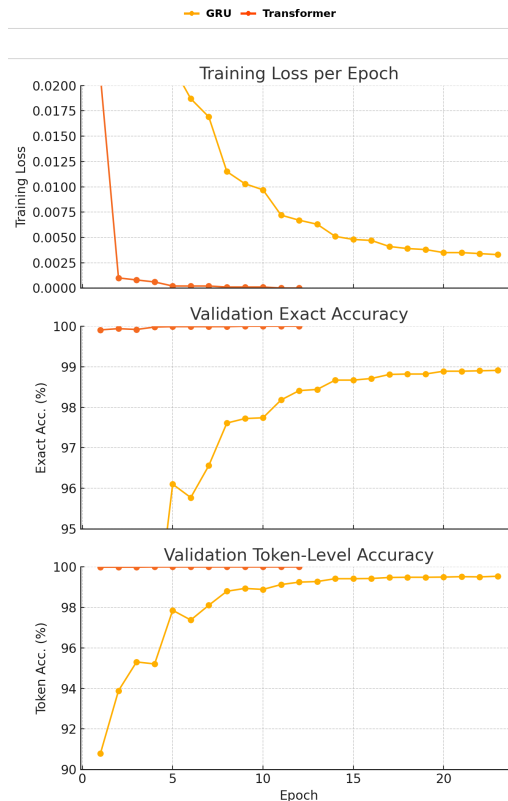


Figure 11. Validation loss and accuracy comparison between the Transformer and GRU-based autoencoders. RNN-AE in the figure represents the GRU-based auto-encoder.

Table 7. Autoencoder reconstruction accuracy on the validation and test set.

Model	Validation		Test	
	Exact (%)	Token (%)	Exact (%)	Token (%)
GRU Autoencoder	98.91	99.54	98.92	99.52
Transformer Autoenc.	100.00	100.00	100.00	100.00

Analysis of Results. The primary source of failure for the GRU was ordering errors, where it produced the correct set of tokens but in an incorrect order. A detailed analysis showed that 9.8% of the GRU’s reconstructions had a non-zero edit distance from the ground truth, typically due to misplaced parentheses or swapped sibling nodes in the expression tree. This confirms the hypothesis that the GRU’s sequential processing and fixed-length hidden state are insufficient to reliably preserve the long-range structural information of complex IRs. The Transformer’s self-attention mechanism, in contrast, processes all tokens in parallel, allowing it to directly model these dependencies and achieve lossless reconstruction. These results validate our choice of the Transformer encoder for state representation.

Table 6. Comparison between four configurations: 1) an initial, naive, implementation of the benchmarks; 2) CHEHAB RL; 3) Coyote; 4) CHEHAB RL with data layout transformation applied after encryption. We compare them in terms of circuit depth (U) and multiplicative depth (U^{\otimes}), number of ciphertext-ciphertext multiplications (\otimes), number of rotations (\cup), number of ciphertext-plaintext multiplications (\odot), and number of ciphertext additions (\oplus). We also report CHEHAB’s and Coyote’s compilation times CT (s) and their Consumed Noise (CN). The important columns in the Table are in bold.

Kernel	Initial						CHEHAB RL						Coyote						CHEHAB RL with data layout transformed after encryption										
	U	U^{\otimes}	\otimes	\cup	\odot	\oplus	U	U^{\otimes}	\otimes	\cup	\odot	\oplus	CN	CT	U	U^{\otimes}	\otimes	\cup	\odot	\oplus	CN	CT	U	U^{\otimes}	\otimes	\cup	\odot	\oplus	CT
Box Blur 3 × 3	9	0	0	0	0	31	6	0	0	1	0	6	13.0	9.57	25	0	0	18	45	24	141.0	471.991	16	1	30	13	30	35	10.568
Box Blur 4 × 4	9	0	0	0	0	74	5	0	0	1	0	5	12.0	10.146	36	0	0	51	111	26	247.0	926.780	15	1	31	13	31	34	9.997
Box Blur 5 × 5	9	0	0	0	0	135	4	0	0	0	0	8	10.0	10.457	36	0	0	100	204	27	250.0	1553.897	10	1	29	8	29	33	10.129
Dot Product 4	5	1	4	0	0	4	6	1	1	3	0	2	45.0	9.826	7	1	1	2	4	4	42.0	106.571	13	2	7	8	6	7	9.21
Dot Product 8	9	1	8	0	0	8	8	1	1	4	0	3	47.0	9.864	9	1	1	3	4	6	93.0	179.196	15	2	7	9	6	8	9.417
Dot Product 16	17	1	16	0	0	16	10	1	1	5	0	4	47.0	11.068	15	1	1	10	14	11	119.0	324.983	29	2	19	22	18	21	11.162
Dot Product 32	33	1	32	0	0	32	11	1	1	5	0	5	44.0	20.492	22	1	1	21	34	16	145.0	629.485	21	2	19	21	18	21	20.536
Hamm. Dist. 4	7	2	8	0	4	8	8	2	2	4	0	3	74.0	9.421	3	2	2	0	0	1	99.0	144.852	14	3	16	12	14	16	9.319
Hamm. Dist. 8	11	2	16	0	8	16	10	2	2	5	0	4	74.0	11.416	4	2	2	3	0	1	73.0	282.906	16	3	16	13	14	17	11.365
Hamm. Dist. 16	19	2	32	0	16	32	12	2	2	6	0	5	75.0	29.736	12	2	2	21	42	12	233.0	520.420	30	3	40	30	38	42	29.816
Hamm. Dist. 32	35	2	64	0	32	64	14	2	3	5	0	7	76.0	178.241	12	2	2	69	92	8	156.0	1054.597	21	3	41	21	38	43	176.251
L2 Distance 4	5	1	4	0	0	3	8	1	1	4	0	2	45.0	9.445	8	1	1	2	4	4	68.0	158.341	21	2	13	15	12	13	9.321
L2 Distance 8	9	1	8	0	0	7	9	1	1	4	0	3	45.0	10.35	11	1	2	3	9	9	122.0	276.027	16	2	13	14	12	13	10.351
L2 Distance 16	17	1	16	0	0	15	11	1	1	5	0	4	46.0	20.696	22	1	2	23	52	18	176.0	574.150	28	2	33	35	32	34	20.735
L2 Distance 32	33	1	32	0	0	31	12	1	1	5	0	5	45.0	95.935	26	1	1	73	101	17	179.0	1170.184	22	2	19	21	18	21	95.549
Linear Reg. 4	3	1	4	0	4	8	5	1	1	2	0	2	41.0	9.36	3	1	1	0	0	0	41.0	2.278	8	2	3	3	2	4	8.995
Linear Reg. 8	3	1	8	0	8	16	5	1	1	2	0	2	41.0	9.469	6	1	1	1	6	3	66.0	197.718	8	2	3	3	2	4	9.312
Linear Reg. 16	3	1	16	0	16	32	4	1	1	1	0	2	41.0	9.547	12	1	1	17	25	7	122.0	500.449	7	2	3	2	2	4	9.283
Linear Reg. 32	3	1	32	0	32	64	3	1	1	0	1	2	10.0	9.778	12	1	1	44	46	4	124.0	963.687	4	2	3	0	3	2	9.466
Poly. Reg. 4	5	2	12	0	0	12	8	2	2	3	0	3	74.0	10.139	16	2	3	4	19	10	153.0	238.869	14	3	8	8	6	9	9.955
Poly. Reg. 8	5	2	24	0	0	24	7	2	2	2	0	3	73.0	9.786	20	2	2	21	38	12	205.0	501.163	10	3	5	4	3	5	9.694
Poly. Reg. 16	5	2	48	0	0	48	6	2	2	1	0	3	73.0	9.993	20	2	2	56	79	12	208.0	961.519	9	3	7	5	5	7	10.06
Poly. Reg. 32	5	2	96	0	0	96	5	2	2	0	0	3	73.0	10.145	20	2	2	134	173	12	210.0	1896.952	6	3	7	0	5	3	9.952
Gx 3 × 3	4	1	24	0	24	36	8	2	4	1	2	6	66.0	9.463	16	1	1	27	57	11	150.0	594.926	12	3	18	9	16	20	9.363
Gx 4 × 4	4	1	48	0	48	64	6	1	3	1	1	4	42.0	10.743	16	1	1	59	112	11	150.0	1061.439	12	2	16	9	14	17	10.599
Gx 5 × 5	4	1	80	0	80	100	5	1	3	0	2	5	40.0	10.646	16	1	1	105	182	12	154.0	1673.958	9	2	16	6	15	16	10.675
Gy 3 × 3	4	1	24	0	24	33	6	1	3	1	1	3	41.0	9.68	16	1	1	29	54	10	149.0	595.976	14	2	20	11	18	20	9.737
Gy 4 × 4	4	1	48	0	48	64	6	1	3	1	0	3	42.0	10.591	16	1	1	60	101	11	197.0	1057.486	14	2	23	11	20	23	10.988
Gy 5 × 5	4	1	80	0	80	105	6	1	5	0	0	6	42.0	11.322	17	1	1	103	169	11	154.0	1670.887	11	2	25	6	20	26	11.197
Rob. Cross 3 × 3	6	2	42.0	0.0	24.0	63.0	5	1	2	2	0	3	45.0	9.786	12	1	2	10	27	11	96.0	291.833	11	2	12	9	10	12	9.661
Rob. Cross 4 × 4	6	2	76.0	0.0	44.0	112.0	5	1	2	2	0	3	44.0	10.363	12	1	2	24	51	9	125.0	543.704	11	2	12	9	10	12	10.133
Rob. Cross 5 × 5	6	2	120.0	0.0	70.0	175.0	4	1	2	0	0	4	42.0	11.681	12	1	2	43	95	10	126.0	857.648	8	2	9	3	7	10	11.505
Mat. Mul. 3 × 3	3	1	27	0	0	18	4	1	2	1	0	2	41.0	9.426	9	1	2	9	14	5	93.0	456.644	11	2	19	11	17	17	9.452
Mat. Mul. 4 × 4	4	1	64	0	0	48	4	1	2	1	0	2	42.0	10.039	10	1	2	32	44	7	94.0	1085.128	13	2	30	16	28	26	9.952
Mat. Mul. 5 × 5	5	1	125	0	0	100	4	1	5	0	0	4	42.0	11.601	14	1	1	69	82	13	145.0	2158.145	10	2	55	16	50	44	11.324
Max 3	6	2	6	0	0	6	9	2	3	3	0	4	76.0	9.481	14	2	3	3	10	9	75.0	132.890	9	2	3	3	0	4	9.481
Max 4	8	3	12	0	0	12	11	3	7	3	0	8	107.0	11.784	22	3	6	8	25	16	235.0	252.436	11	3	7	3	0	8	11.784
Max 5	10	4	20	0	0	20	15	4	12	5	0	12	140.0	149.936	29	4	9	27	55	21	321.0	509.189	15	4	12	5	0	12	149.936
Sort 3	8	3	10	0	0	8	11	3	5	3	0	6	107.0	10.552	12	3	4	5	6	9	188.0	184.944	11	3	5	3	0	6	10.552
Sort 4	14	6	58	0	0	35	21	6	26	5	0	35	206.0	522.043	42	6	10	66	114	31	369.0	959.704	21	6	26	5	0	35	522.043
Tree 50-50-5	4	2	2.0	0.0	0.0	4.0	8	2	2	3	0	3	73.0	9.271	4	2	0	0	4	73.0	4.306	8	2	2	3	0	3	9.271	
Tree 50-50-10	10	5	16.0	0.0	0.0	16.0	15	5	15	2	0	18	172.0	18.17	27	7	7	7	19	21	243.0	147.033	15	5	15	2	0	18	18.17
Tree 100-50-5	5	3	15.0	0.0	0.0	16.0	13	5	8	3	0	13	169.0	12.428	18	3	4	7	22	14	212.0	176.904	13	5	8	3	0	13	12.428
Tree 100-50-10	10	8	519.0	0.0	0.0	504.0	16	8	509	2	0	511	334.0	148.398	50	8	148	490	873	243	369.0	6798.692	16	8	509	2	0	511	148.398
Tree 100-100-5	5	4	29.0	0.0	0.0	2.0	10	4	4	5	0	1	141.0	11.152	16	5	5	5	13	7	211.0	170.154	10	4	4	5	0	1	11.152
Tree 100-100-10	10	9	1022.0	0.0	0.0	1.0	12	9	256	2	0	1	307.0	91.627	36	10	10	334	373	16	369.0	5396.742	1						

vectorized code [73], which affects its ability to take advantage of SIMD parallelism and improve latency. HECATE [49] is a recent work that focuses on selecting the parameter q for CKKS, and at the same time it performs ciphertext-maintenance operations scheduling by applying rewrite on the input circuit, HECATE outperforms EVA by 27.38%, however, it does not apply any optimization to reduce the number of operations and multiplicative depth of the circuit.

RL-based methods for Code Optimization. Recent attempts explored the use of reinforcement learning to solve the problem of choosing the right sequence of code transformations. In PolyGym [17] and CompilerGym [25], the authors propose only RL environments without implementing RL agents to optimize code; their main contribution is to show that their action space has potentially good optimizations to explore. They leave the implementation of an RL agent as future work.

Other work such as HalideRL [59], AutoPhase [37] and SuperSonic [40] propose RL agents to optimize code. HalideRL is not fully automatic. The user has to provide an initial set of code transformations. The HalideRL agent then discards transformations that are not useful and keeps only those that are useful. It then selects the best parameters for the useful transformations. In addition, HalideRL does not generalize to programs unseen during training. It is trained on a given program with multiple random data input sizes. Then, during deployment, it is used to optimize that same program. This is different from our approach. Our RL agent is designed to generalize to programs unseen during training. We train our RL agent on a large set of random LLM-generated programs. Once it learns how to optimize them, we then deploy it on new unseen programs and use it to optimize them.

SuperSonic [40] is a meta-optimizer that targets the problem of choosing the best RL algorithm and the best representation of states and actions, while AutoPhase [37] targets the problem of phase ordering, i.e., selecting the best order for compiler passes.

While previous work addresses traditional code optimizations, it does not consider the unique constraints of FHE. Our work is the first to formulate FHE optimization as an RL problem, where the agent must learn a policy that navigates the trade-offs between vectorization, cryptographic noise accumulation, and the cost of operations.

Tokenization and Variable Renaming. Tokenization has been widely used in NLP. Classical NLP moved from word-level tokenization to learned subword units, with methods such as *Byte-Pair Encoding* (BPE) [65]; more recently, tokenization-free methods process raw characters or bytes (e.g., *CANINE* [22]), which eliminates vocabulary design but lengthens sequences and shifts compute into the model. In coding tasks, BPE has been widely used as a tokenization

method for models that take code as input in its textual format (e.g. *CodeBERT* [33]). None of these methods applies variable renaming at the tokenization level, though.

Variable renaming to obtain canonical representations of code was explored for classical clone detection, as in *CCFinder* [44]. Such variable renaming was not used as a tokenization method for deep learning models, though.

Our approach differs from the previous approaches. We normalize the IR by replacing variable names and numeric constants with generic tokens, since their exact values do not affect our rewrite rules, which means that our tokenization method is more specific to our use case. This makes it faster to learn than BPE but still preserves the structural signals the model needs.

Random Code Generation. Random code generation is a common strategy for constructing training corpora for learning-based compiler optimization. Systems such as the Tiramisu autoscheduler [9], Looper [55], and the Halide autoscheduler [1] use stochastic code generators in which the probabilities of syntactic and semantic patterns are manually specified to sample diverse code patterns. To eliminate this manual specification burden, Cummins et al. [24] learn a generative model from large-scale real-world code and then sample synthetic programs whose distribution better matches human-written code. More recently, PIE [66] and EfiCoder [39] use large language models (LLMs) to synthesize code that is subsequently used to train or fine-tune downstream models for performance-oriented code optimization. Our approach follows this latter line: we leverage an off-the-shelf, pretrained LLM, already exposed to the distribution of real-world code, to synthesize training programs, thereby avoiding task-specific generator design and hand-tuning of pattern priors.

K Frequently Asked Questions

In this section, we provide a list of frequently asked questions and answers to these questions. These provide more clarification about the paper.

- **Examples of end-user deployments for homomorphic encryption** End-user deployments for homomorphic encryption have already appeared: for example, Microsoft Edge’s Password Monitor uses homomorphic encryption to check user credentials against breach corpora without revealing inputs [48, 72]. Beyond credentials checking, homomorphic encryption is being used in sensitive scientific/health settings (e.g., private genotype imputation and kinship detection in genomics), both reporting practical runtimes on real datasets [35, 46]. The UK Information Commissioner’s Office documents a cross-institution deployment in which banks and law-enforcement agencies use homomorphic encryption to run encrypted queries to detect financial crime [41].

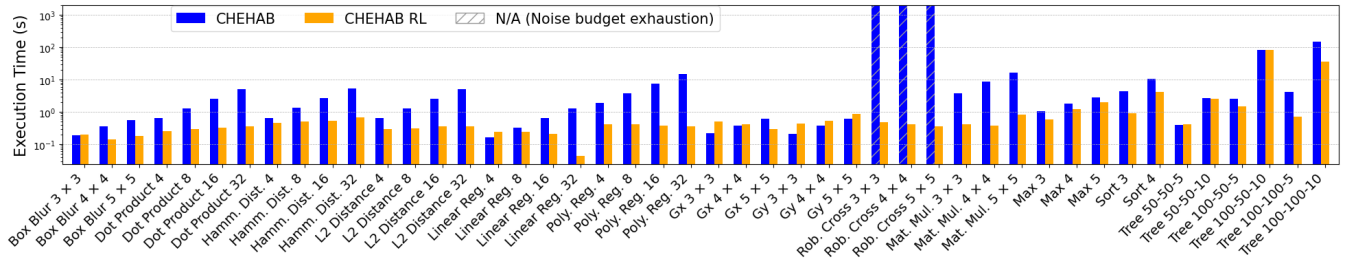


Figure 12. Semi-log plots comparing the execution times of the default CHEHAB and CHEHAB RL.

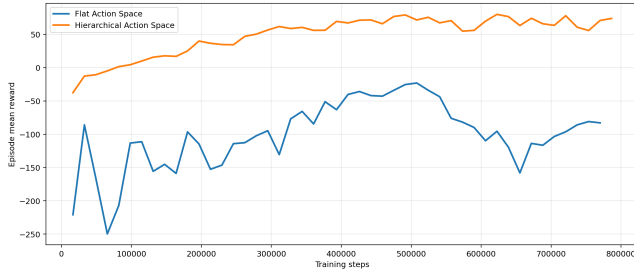


Figure 13. Graph comparing Episode Mean Reward Over Timesteps of Flat vs. Hierarchical Action Spaces.

- **Why not use an LLM to directly optimize CHEHAB IR at inference time?** It is an interesting direction. In this work, our goal is *fast and deterministic* compilation, which favors an RL policy evaluated locally inside the compiler. At inference time, the RL agent produces a rewrite sequence in a few seconds with stable runtime and fully reproducible behavior. In contrast, LLM-based optimization at inference time typically incurs substantially higher latency and cost, and can be less predictable due to sampling and the need for output validation/repair. For example, the ComPilot paper [56] reports an average of 8 minutes to optimize a single loop nest.

L Artifact Appendix

L.1 Abstract

CHEHAB is a fully homomorphic encryption (FHE) compiler that translates a domain-specific language into Microsoft SEAL (BFV) programs and applies optimization passes including a reinforcement-learning-guided rewrite selection, constant folding and common subexpression elimination. The artifact reproduces the key results of our paper (Table 6, Figure 5) by running the benchmark suite (e.g., Box Blur, Dot Product, Hamming Distance, L2 Distance, Linear/Polynomial Regression, Matrix Multiplication, Max, Sort, and polynomial-tree benchmarks) under the same optimization configurations used in the evaluation, and collecting compile-time and execution-time metrics as well as circuit-level properties (depth, multiplicative depth, remaining noise budget, and operation counts). The workflow produces CSV result

files in `results/` and includes scripts to generate the corresponding plots from these CSVs. The artifact is packaged with a ready-to-use Docker environment (Ubuntu + SEAL + Conda dependencies) for interactive use of the compiler, and an optional web interface for running individual benchmark configurations and inspecting logs and optimized expressions.

L.2 Artifact check-list (meta-information)

- **Algorithm:** RL-guided optimization for FHE compilation (learned rewrite selection)
- **Program:** C++ compiler + benchmarks, Python benchmark driver, optional FastAPI web UI
- **Compilation:** CMake, GCC/G++, Microsoft SEAL (BFV)
- **Transformations:** RL-guided rewrite selection, constant folding, common subexpression elimination
- **Binary:** benchmark executables in `build/benchmarks/<bench>/HE runner main` in generated `he/`
- **Model:** RL agent code under `RL/fhe_rl/` (trained models included)
- **Data set:** LLM-generated dataset used for training (no external dataset)
- **Run-time environment:** Docker (Ubuntu 22.04) + Conda env `chehabEnv`; optional host install per README
- **Hardware:** x86_64 CPU, ≥ 32 GB RAM recommended, for our experiments we used 1 node, 32 cores, 128 GB RAM
- **Execution:** `pythonrun_benchmarks.py` (RL mode); optional `dockercomposeupchehab-demo` for web UI
- **Metrics:** compile time, execution time, depth, multiplicative depth, remaining noise budget, operation counts
- **Output:** CSV files in `results/`; optional plots (PNG) from `results/generate_graphs.py`
- **Experiments:** benchmark suite runs across multiple slot counts and RL settings; per-benchmark runs via CLI or web UI
- **How much disk space required (approximately)?:** 25-30 GB (Docker image + build + outputs)
- **How much time is needed to prepare workflow (approximately)?:** 45-60 minutes (first Docker build)
- **How much time is needed to complete experiments (approximately)?:** 45-90 minutes (depends on iterations)
- **Publicly available?:** Yes
- **Workflow automation framework used?:** Python scripts, Docker Compose

L.3 Description

L.3.1 How to access. The artifact is available as a public repository: <https://github.com/Modern-Compilers-Lab/CHEHAB>. A Docker-based environment is provided for reproducible setup and execution. A host-native installation is also possible by following the repository README (including Microsoft SEAL and toolchain installation).

L.3.2 Software dependencies. Recommended: Docker and Docker Compose. The Docker image includes Ubuntu 22.04, Microsoft SEAL, the required build toolchain, and a Conda environment (chehabEnv) with Python dependencies used by the RL optimization pipeline.

L.4 Installation

Build the interactive environment. From the repository root, build the interactive environment:

```
$ docker compose build chehab-main
```

Build the web UI service (optional). From the repository root, build the web UI service:

```
$ docker compose build chehab-demo
```

Host setup (optional). If you prefer running without Docker, follow the README for the complete host installation procedure (including Microsoft SEAL and all required dependencies).

L.5 Experiment workflow

CLI workflow (recommended). Launch an interactive container shell:

```
$ docker compose run --rm -it \
  chehab-main /bin/bash
```

The Docker image is configured to auto-activate chehabEnv for interactive bash shells. If it is not active, run:

```
$ source /opt/conda/etc/profile.d/conda.sh
$ conda activate chehabEnv
```

Run the benchmark suite:

```
$ python run_benchmarks.py
```

The script writes the results as CSV files in `results/`, this directory is bind-mounted, so the files are mirrored to the local `results/` folder on the host.

Web workflow (optional). Start the web service:

```
$ docker compose up chehab-demo
```

Then open <http://localhost:8000> to run individual benchmark configurations and inspect logs.

L.6 Evaluation and expected results

Successful execution produces CSV result files in `results/`. Each row corresponds to a benchmark configuration and reports compile-time and execution-time measurements, along with circuit-level statistics (e.g., depth, multiplicative depth, remaining noise budget, and operation counts). Optional plots can be generated from the CSV outputs using `generate_graphs.py`. A file such as `results/results_RL.csv` is produced. To generate an execution-time plot:

```
$ python results/generate_graphs.py \
  --metric exec \
  --csv results/results_RL.csv \
  --label "CHEHAB RL" \
  --output results/exec_time.png
```

To plot remaining noise budget:

```
$ python results/generate_graphs.py \
  --metric noise \
  --csv results/results_RL.csv \
  --label "CHEHAB RL" \
  --output results/noise_budget.png
```

L.7 Experiment customization

The benchmark sweep parameters (e.g., slot counts, number of iterations, and timeouts) can be modified in `run_benchmarks.py`. When using Docker Compose, `run_benchmarks.py` is bind-mounted into the container, so changes are mirrored immediately and do not require rebuilding the image. The web UI exposes common parameters directly in its input form.

RL-specific customization is done in `RL/fhe_rl/config.py`, which selects the RL model to use, for example, users can switch to the agent trained with the random dataset by changing the configured model path. This file is also bind-mounted in the Docker workflow, so edits take effect without rebuilding.

L.8 Notes

The Docker workflow is recommended to avoid dependency and toolchain mismatches. If running outside Docker, follow the README to install Microsoft SEAL and all dependencies.

References

- [1] Andrew Adams, Karima Ma, Luke Anderson, Riyadh Baghdadi, Tzu-Mao Li, Michaël Gharbi, Benoit Steiner, Steven Johnson, Kayvon Fatahalian, Frédo Durand, and Jonathan Ragan-Kelley. 2019. Learning to optimize halide with tree search and random programs. *ACM Trans. Graph.* 38, 4, Article 121 (July 2019), 12 pages. doi:10.1145/3306346.3322967
- [2] Alfred V. Aho, Monica S. Lam, Ravi Sethi, and Jeffrey D. Ullman. 2006. *Compilers: Principles, Techniques, and Tools* (2 ed.). Addison-Wesley, Boston, MA, USA.
- [3] Martin Albrecht, Melissa Chase, Hao Chen, Jintai Ding, Shafi Goldwasser, Sergey Gorbunov, Shai Halevi, Jeffrey Hoffstein, Kim Laine, Kristin Lauter, Satya Lokam, Daniele Micciancio, Dustin Moody, Travis

- Morrison, Amit Sahai, and Vinod Vaikuntanathan. 2019. Homomorphic Encryption Standard. Cryptology ePrint Archive, Paper 2019/939. <https://eprint.iacr.org/2019/939>
- [4] Asra Ali, Jaeho Choi, Bryant Gipson, Shruthi Gorantala, Jeremy Kun, Wouter Legiest, Lawrence Lim, Alexander Viand, Meron Zerihun Demissie, and Hongren Zheng. 2025. HEIR: A Universal Compiler for Homomorphic Encryption. arXiv:2508.11095 [cs.CR]. arXiv:2508.11095 [cs.CR]
- [5] David W. Archer, José Manuel Calderón Trilla, Jason Dagit, Alex Malozemoff, Yuriy Polyakov, Kurt Rohloff, and Gerard Ryan. 2019. RAMPARTS: A Programmer-Friendly System for Building Homomorphic Encryption Applications. In *Proceedings of the 7th ACM Workshop on Encrypted Computing & Applied Homomorphic Cryptography* (London, United Kingdom) (WAHC'19). Association for Computing Machinery, New York, NY, USA, 57–68. doi:10.1145/3338469.3358945
- [6] Frederik Armknecht, Colin Boyd, Christopher Carr, Kristian Gjøsteen, Angela Jäschke, Christian A Reuter, and Martin Strand. 2015. A guide to fully homomorphic encryption. Cryptology ePrint Archive, Paper 2015/1192. <https://eprint.iacr.org/2015/1192>.
- [7] Amir H. Ashouri, Mostafa Elhoushi, Yuzhe Hua, Xiang Wang, Muhammad Asif Manzoor, Bryan Chan, and Yaoqing Gao. 2022. Work-in-Progress: MLGPerf: An ML Guided Inliner to Optimize Performance. In *2022 International Conference on Compilers, Architecture, and Synthesis for Embedded Systems (CASES)*. 3–4. doi:10.1109/CASES55004.2022.00008
- [8] Riyadh Baghdadi. 2015. *Improving tiling, reducing compilation time, and extending the scope of polyhedral compilation*. Ph. D. Dissertation. Paris 6.
- [9] Riyadh Baghdadi, Massinissa Merouani, Mohamed-Hicham Leghettas, Kamel Abdous, Taha Arbaoui, Karima Benatchba, and Saman Amarasinghe. 2021. A Deep Learning Based Cost Model for Automatic Code Optimization. arXiv:2104.04955 [cs.PL] <https://arxiv.org/abs/2104.04955>
- [10] Riyadh Baghdadi, Jessica Ray, Malek Ben Romdhane, Emanuele Del Sozzo, Abdurrahman Akkas, Yunming Zhang, Patricia Suriana, Shoaib Kamil, and Saman Amarasinghe. 2019. Tiramisu: a polyhedral compiler for expressing fast and portable code. In *Proceedings of the 2019 IEEE/ACM International Symposium on Code Generation and Optimization* (Washington, DC, USA) (CGO 2019). IEEE Press, Piscataway, NJ, USA, 193–205.
- [11] Riyadh Baghdadi, Jessica Ray, Malek Ben Romdhane, Emanuele Del Sozzo, Patricia Suriana, Shoaib Kamil, and Saman P Amarasinghe. 2018. Tiramisu: A code optimization framework for high performance systems. arXiv preprint arXiv:1804.10694 (2018).
- [12] Uday Bondhugula, Albert Hartono, J. Ramanujam, and P. Sadayappan. 2008. A practical automatic polyhedral parallelizer and locality optimizer. *SIGPLAN Not.* 43, 6 (June 2008), 101–113. doi:10.1145/1379022.1375595
- [13] Uday Bondhugula, Albert Hartono, J. Ramanujam, and P. Sadayappan. 2008. A practical automatic polyhedral parallelizer and locality optimizer. In *PLDI*. 101–113.
- [14] Zvika Brakerski. 2012. Fully Homomorphic Encryption without Modulus Switching from Classical GapSVP. In *Advances in Cryptology – CRYPTO 2012*, Reihaneh Safavi-Naini and Ran Canetti (Eds.). Springer Berlin Heidelberg, Berlin, Heidelberg, 868–886.
- [15] Zvika Brakerski, Craig Gentry, and Vinod Vaikuntanathan. 2012. (Leveled) fully homomorphic encryption without bootstrapping. In *Proceedings of the 3rd Innovations in Theoretical Computer Science Conference* (Cambridge, Massachusetts) (ITCS '12). Association for Computing Machinery, New York, NY, USA, 309–325. doi:10.1145/2090236.2090262
- [16] Alexander Brauckmann, Andrés Goens, and Jeronimo Castrillon. 2021. PolyGym: Polyhedral Optimizations as an Environment for Reinforcement Learning. In *Proceedings of the 30th International Conference on Parallel Architectures and Compilation Techniques* (Atlanta, GA, USA) (PACT '21). IEEE Press, Piscataway, NJ, USA, 17–29. doi:10.1109/PACT52795.2021.00009
- [17] Alexander Brauckmann, Andrés Goens, and Jeronimo Castrillon. 2021. A reinforcement learning environment for polyhedral optimizations. arXiv preprint arXiv:2104.13732.
- [18] Tianqi Chen, Lianmin Zheng, Eddie Yan, Ziheng Jiang, Thierry Moreau, Luis Ceze, Carlos Guestrin, and Arvind Krishnamurthy. 2018. Learning to optimize tensor programs. In *Advances in Neural Information Processing Systems*. 3389–3400.
- [19] Yishen Chen, Charith Mendis, Michael Carbin, and Saman Amarasinghe. 2021. VeGen: a vectorizer generator for SIMD and beyond. In *Proceedings of the 26th ACM International Conference on Architectural Support for Programming Languages and Operating Systems* (Virtual, USA) (ASPLOS '21). Association for Computing Machinery, New York, NY, USA, 902–914. doi:10.1145/3445814.3446692
- [20] Eduardo Chielle, Oleg Mazonka, Homer Gamil, Nektarios Georgios Tsoutsos, and Michail Maniatakos. 2018. E3: A Framework for Compiling C++ Programs with Encrypted Operands. Cryptology ePrint Archive, Paper 2018/1013. <https://eprint.iacr.org/2018/1013>
- [21] Sangeeta Chowdhary, Wei Dai, Kim Laine, and Olli Saarikivi. 2021. EVA Improved: Compiler and Extension Library for CKKS. Cryptology ePrint Archive, Paper 2021/1505. doi:10.1145/3474366.3486929 <https://eprint.iacr.org/2021/1505>.
- [22] Jonathan H. Clark, Dan Garrette, Iulia Turc, and John Wieting. 2022. Canine: Pre-training an Efficient Tokenization-Free Encoder for Language Representation. *Transactions of the Association for Computational Linguistics* 10 (2022), 73–91. doi:10.1162/tacl_a_00448
- [23] Meghan Cowan, Deeksha Dangwal, Armin Alaghi, Caroline Trippel, Vincent T. Lee, and Brandon Reagen. 2021. Porcupine: A Synthesizing Compiler for Vectorized Homomorphic Encryption. In *Proceedings of the 42nd ACM SIGPLAN International Conference on Programming Language Design and Implementation* (Virtual, Canada) (PLDI 2021). Association for Computing Machinery, New York, NY, USA, 375–389. doi:10.1145/3453483.3454050
- [24] Chris Cummins, Pavlos Petoumenos, Zheng Wang, and Hugh Leather. 2017. Synthesizing benchmarks for predictive modeling. In *2017 IEEE/ACM International Symposium on Code Generation and Optimization (CGO)*. IEEE Press, Piscataway, NJ, USA, 86–99. doi:10.1109/CGO.2017.7863731
- [25] Chris Cummins, Bram Wasti, Jiadong Guo, Brandon Cui, Jason Ansel, Sahir Gomez, Somya Jain, Jia Liu, Olivier Teytaud, Benoit Steiner, Yuandong Tian, and Hugh Leather. 2022. CompilerGym: robust, performant compiler optimization environments for AI research. In *Proceedings of the 20th IEEE/ACM International Symposium on Code Generation and Optimization* (Virtual Event, Republic of Korea) (CGO '22). IEEE Press, Piscataway, NJ, USA, 92–105. doi:10.1109/CGO53902.2022.9741258
- [26] Roshan Dathathri, Blagovesta Kostova, Olli Saarikivi, Wei Dai, Kim Laine, and Madan Musuvathi. 2020. EVA: An Encrypted Vector Arithmetic Language and Compiler for Efficient Homomorphic Computation. In *Proceedings of the 41st ACM SIGPLAN Conference on Programming Language Design and Implementation* (London, UK) (PLDI 2020). Association for Computing Machinery, New York, NY, USA, 546–561. doi:10.1145/3385412.3386023
- [27] Roshan Dathathri, Olli Saarikivi, Hao Chen, Kim Laine, Kristin Lauter, Saeed Maleki, Madanlal Musuvathi, and Todd Mytkowicz. 2019. CHET: An Optimizing Compiler for Fully-Homomorphic Neural-Network Inferencing. In *Proceedings of the 40th ACM SIGPLAN Conference on Programming Language Design and Implementation* (Phoenix, AZ, USA) (PLDI 2019). Association for Computing Machinery, New York, NY, USA, 142–156. doi:10.1145/3314221.3314628
- [28] Jacob Devlin, Ming-Wei Chang, Kenton Lee, and Kristina Toutanova. 2019. BERT: Pre-training of Deep Bidirectional Transformers for Language Understanding. In *Proceedings of the 2019 Conference of the*

- North American Chapter of the Association for Computational Linguistics: Human Language Technologies, Volume 1 (Long and Short Papers)*, Jill Burstein, Christy Doran, and Thamar Solorio (Eds.). Association for Computational Linguistics, Minneapolis, Minnesota, 4171–4186. doi:10.18653/v1/N19-1423
- [29] David Steven Dummit and Richard M Foote. 2004. *Abstract Algebra*. Vol. 3. John Wiley & Sons, Hoboken, NJ.
- [30] Austin Ebel, Karthik Garimella, and Brandon Reagen. 2025. Orion: A Fully Homomorphic Encryption Framework for Deep Learning. In *Proceedings of the 30th ACM International Conference on Architectural Support for Programming Languages and Operating Systems, Volume 2 (ASPLOS '25)*. ACM, New York, NY, USA, Article 16, 16 pages. arXiv:arXiv:2311.03470v3 doi:10.1145/3676641.3716008
- [31] Alexandre E. Eichenberger, Peng Wu, and Kevin O'Brien. 2004. Vectorization for SIMD architectures with alignment constraints. *SIGPLAN Not.* 39, 6 (June 2004), 82–93. doi:10.1145/996893.996853
- [32] Junfeng Fan and Frederik Vercauteren. 2012. Somewhat Practical Fully Homomorphic Encryption. Cryptology ePrint Archive, Paper 2012/144. <https://eprint.iacr.org/2012/144>
- [33] Zhangyin Feng, Daya Guo, Duyu Tang, Nan Duan, Xiaocheng Feng, Ming Gong, Linjun Shou, Bing Qin, Ting Liu, Daxin Jiang, and Ming Zhou. 2020. CodeBERT: A Pre-Trained Model for Programming and Natural Languages. In *Findings of the Association for Computational Linguistics: EMNLP 2020*, Trevor Cohn, Yulan He, and Yang Liu (Eds.). Association for Computational Linguistics, Online, 1536–1547. doi:10.18653/v1/2020.findings-emnlp.139
- [34] Tobias Grosser, Armin Groslinger, and Christian Lengauer. 2012. Polly - Performing Polyhedral Optimizations on a Low-Level Intermediate Representation. *Parallel Processing Letters* 22, 4 (2012). <http://dblp.uni-trier.de/db/journals/ppl/ppl22.html#GrosserGL12>
- [35] Gamze Gürsoy, Eduardo Chielle, Charlotte M Brannon, Michail Maniatakos, and Mark Gerstein. 2022. Privacy-preserving genotype imputation with fully homomorphic encryption. *Cell systems* 13, 2 (2022), 173–182.
- [36] Ameer Haj-Ali, Nesreen K. Ahmed, Ted Willke, Yakun Sophia Shao, Krste Asanovic, and Ion Stoica. 2020. NeuroVectorizer: end-to-end vectorization with deep reinforcement learning. In *Proceedings of the 18th ACM/IEEE International Symposium on Code Generation and Optimization (San Diego, CA, USA) (CGO '20)*. Association for Computing Machinery, New York, NY, USA, 242–255. doi:10.1145/3368826.3377928
- [37] Ameer Haj-Ali, Qijing Huang, John Xiang, William Moses, Ion Stoica, Krste Asanovic, and John Wawrzyniek. 2020. AutoPhase: Juggling HLS Phase Orderings in Random Forests with Deep Reinforcement Learning. In *Proceedings of the 3rd Conference on Machine Learning and Systems (MLSys '20)*, Vol. 2. mlsys.org, Austin, TX, USA, 177–202. <https://proceedings.mlsys.org/papers/2020/26>
- [38] Yacine Hakimi, Riyadh Baghdadi, and Yacine Challal. 2023. A hybrid machine learning model for code optimization. *International Journal of Parallel Programming* 51, 6 (2023), 309–331.
- [39] Dong Huang, Guangtao Zeng, Jianbo Dai, Meng Luo, Han Weng, Yuhao Qing, Heming Cui, Zhijiang Guo, and Jie M. Zhang. 2025. EffiCoder: Enhancing Code Generation in Large Language Models through Efficiency-Aware Fine-tuning. arXiv:2410.10209 [cs.CL] <https://arxiv.org/abs/2410.10209>
- [40] Wang Huanting, Tang Zhanyong, Zhang Cheng, Zhao Jiaqi, Cummins Chris, Leather Hugh, and Wang Zheng. 2022. Automating Reinforcement Learning Architecture Design for Code Optimization. In *Proceedings of the 31st ACM SIGPLAN International Conference on Compiler Construction (Seoul, South Korea) (CC 2022)*. Association for Computing Machinery, New York, NY, USA, 129–143. doi:10.1145/3497776.3517769
- [41] Information Commissioner's Office. 2023. Case study: homomorphic encryption for data sharing. <https://ico.org.uk/for-organisations/uk-gdpr-guidance-and-resources/data-sharing/privacy-enhancing-technologies/case-studies/homomorphic-encryption-for-data-sharing/> Accessed: 2025-08-17.
- [42] F. Irigoien and R. Triolet. 1988. Supernode Partitioning. In *POPL '88*. San Diego, CA, 319–328.
- [43] Lei Jiang and Lei Ju. 2022. FHEBench: Benchmarking Fully Homomorphic Encryption Schemes. arXiv:2203.00728 [cs.CR] <https://arxiv.org/abs/2203.00728>
- [44] T. Kamiya, S. Kusumoto, and K. Inoue. 2002. CCFinder: a multilingual token-based code clone detection system for large scale source code. *IEEE Transactions on Software Engineering* 28, 7 (2002), 654–670. doi:10.1109/TSE.2002.1019480
- [45] Ken Kennedy and John R. Allen. 2001. *Optimizing compilers for modern architectures: a dependence-based approach*. Morgan Kaufmann Publishers Inc., San Francisco, CA, USA.
- [46] Miran Kim, Arif Ozgun Harmanci, Jean-Philippe Bossuat, Sergiu Carpov, Jung Hee Cheon, Ilaria Chillotti, Wonhee Cho, David Froelicher, Nicolas Gama, Mariya Georgieva, Seungwan Hong, Jean-Pierre Hubaux, Duhyeong Kim, Kristin Lauter, Yiping Ma, Lucila Ohno-Machado, Heidi Sofia, Yongha Son, Yongsoo Song, Juan Troncoso-Pastoriza, and Xiaoqian Jiang. 2021. Ultrafast homomorphic encryption models enable secure outsourcing of genotype imputation. *Cell Systems* 12, 11 (2021), 1108–1120.e4. doi:10.1016/j.cels.2021.07.010
- [47] Samuel Larsen and Saman Amarasinghe. 2000. Exploiting superword level parallelism with multimedia instruction sets. In *Proceedings of the ACM SIGPLAN 2000 Conference on Programming Language Design and Implementation (Vancouver, British Columbia, Canada) (PLDI '00)*. Association for Computing Machinery, New York, NY, USA, 145–156. doi:10.1145/349299.349320
- [48] Kristin Lauter, Sreekanth Kannepalli, Kim Laine, and Radames Cruz Moreno. 2021. Password Monitor: Safeguarding passwords in Microsoft Edge. Microsoft Research Blog. <https://www.microsoft.com/en-us/research/blog/password-monitor-safeguarding-passwords-in-microsoft-edge/> Accessed: 2025-08-17.
- [49] Yongwoo Lee, Seonyeong Heo, Seonyoung Cheon, Shinnung Jeong, Changsu Kim, Eunkyoung Kim, Dongyoon Lee, and Hanjun Kim. 2022. HECATE: Performance-Aware Scale Optimization for Homomorphic Encryption Compiler. In *2022 IEEE/ACM International Symposium on Code Generation and Optimization (CGO)*. IEEE Press, Piscataway, NJ, USA, 193–204. doi:10.1109/CGO53902.2022.9741265
- [50] Long Li, Jianxin Lai, Peng Yuan, Tianxiang Sui, Yan Liu, Qing Zhu, Xiaojing Zhang, Linjie Xiao, Wenguang Chen, and Jingling Xue. 2025. ANT-ACE: An FHE Compiler Framework for Automating Neural Network Inference. In *Proceedings of the 23rd ACM/IEEE International Symposium on Code Generation and Optimization (CGO '25)* (Las Vegas, NV, USA). Association for Computing Machinery, New York, NY, USA, 408–421. doi:10.1145/3696443.3708924
- [51] Vadim Lyubashevsky, Chris Peikert, and Oded Regev. 2013. On Ideal Lattices and Learning with Errors over Rings. *J. ACM* 60, 6, Article 43 (2013), 35 pages.
- [52] Raghav Malik, Kabir Sheth, and Milind Kulkarni. 2023. Coyote: A Compiler for Vectorizing Encrypted Arithmetic Circuits. In *Proceedings of the 28th ACM International Conference on Architectural Support for Programming Languages and Operating Systems, Volume 3 (Vancouver, BC, Canada) (ASPLOS 2023)*. Association for Computing Machinery, New York, NY, USA, 118–133. doi:10.1145/3582016.3582057
- [53] Charith Mendis and Saman Amarasinghe. 2018. goSLP: globally optimized superword level parallelism framework. *Proc. ACM Program. Lang.* 2, OOPSLA, Article 110 (Oct. 2018), 28 pages. doi:10.1145/3276480
- [54] Massinissa Merouani, Khaled Afif Boudaoud, Iheb Nassim Aouadj, Nassim Tchoulak, Islem Kara Bernou, Hamza Benyamina, Fatima Benbouzid-Si Tayeb, Karima Benatchba, Hugh Leather, and Riyadh Baghdadi. 2024. LOOPer: A Learned Automatic Code Optimizer For Polyhedral Compilers. *arXiv preprint arXiv:2403.11522* (2024).

- [55] Massinissa Merouani, Khaled Afif Boudaoud, Iheb Nassim Aouadj, Nassim Tchoulak, Islem Kara Bernou, Hamza Benyamina, Fatima Benbouzid-Si Tayeb, Karima Benatchba, Hugh Leather, and Riyadh Baghdadi. 2025. LOOPer: A Learned Automatic Code Optimizer For Polyhedral Compilers. arXiv:2403.11522 [cs.PL] <https://arxiv.org/abs/2403.11522>
- [56] Massinissa Merouani, Islem Kara Bernou, and Riyadh Baghdadi. 2025. Agentic Auto-Scheduling: An Experimental Study of LLM-Guided Loop Optimization. In *International Conference on Parallel Architectures and Compilation Techniques (PACT)*. IEEE, Piscataway, NJ, USA, 186–200. arXiv:2511.00592 [cs.PL] doi:10.1109/PACT65351.2025.00027
- [57] Microsoft Research. 2023. Microsoft SEAL (release 4.1). <https://github.com/Microsoft/SEAL>. Redmond, WA.
- [58] Julie L. Newcomb, Andrew Adams, Steven Johnson, Rastislav Bodik, and Shoab Kamil. 2020. Verifying and Improving Halide’s Term Rewriting System with Program Synthesis. *Proc. ACM Program. Lang.* 4, OOPSLA, Article 166 (nov 2020), 28 pages. doi:10.1145/3428234
- [59] Marcelo Pecenin, André Maidl, and Daniel Weingaertner. 2019. Optimization of Halide Image Processing Schedules with Reinforcement Learning. In *Proceedings of the 20th Symposium on High Performance Computing Systems (Campo Grande)*. SBC, Porto Alegre, RS, Brasil, 37–48. doi:10.5753/wscad.2019.8655
- [60] Phitchaya Mangpo Phothilimthana, Archibald Samuel Elliott, An Wang, Abhinav Jangda, Bastian Hagedorn, Henrik Barthels, Samuel J. Kaufman, Vinod Grover, Emina Torlak, and Rastislav Bodik. 2019. Swizzle Inventor: Data Movement Synthesis for GPU Kernels. In *Proceedings of the Twenty-Fourth International Conference on Architectural Support for Programming Languages and Operating Systems (Providence, RI, USA) (ASPLOS ’19)*. Association for Computing Machinery, New York, NY, USA, 65–78. doi:10.1145/3297858.3304059
- [61] Antonin Raffin, Ashley Hill, Adam Gleave, Anssi Kanervisto, Maximilian Ernestus, and Noah Dormann. 2021. Stable-Baselines3: Reliable Reinforcement Learning Implementations. *Journal of Machine Learning Research* 22, 268 (2021), 1–8. <http://jmlr.org/papers/v22/20-1364.html>
- [62] Jonathan Ragan-Kelley, Andrew Adams, Dillon Sharlet, Connelly Barnes, Sylvain Paris, Marc Levoy, Saman Amarasinghe, and Frédo Durand. 2017. Halide: decoupling algorithms from schedules for high-performance image processing. *Commun. ACM* 61, 1 (Dec. 2017), 106–115. doi:10.1145/3150211
- [63] Gang Ren, Peng Wu, and David Padua. 2006. Optimizing data permutations for SIMD devices. *SIGPLAN Not.* 41, 6 (June 2006), 118–131. doi:10.1145/1133255.1133996
- [64] John Schulman, Filip Wolski, Prafulla Dhariwal, Alec Radford, and Oleg Klimov. 2017. Proximal Policy Optimization Algorithms. arXiv preprint arXiv:1707.06347. <https://arxiv.org/abs/1707.06347>
- [65] Rico Sennrich, Barry Haddow, and Alexandra Birch. 2016. Neural Machine Translation of Rare Words with Subword Units. In *Proceedings of the 54th Annual Meeting of the Association for Computational Linguistics (Volume 1: Long Papers)*, Katrin Erk and Noah A. Smith (Eds.). Association for Computational Linguistics, Berlin, Germany, 1715–1725. doi:10.18653/v1/P16-1162
- [66] Alexander Shypula, Aman Madaan, Yimeng Zeng, Uri Alon, Jacob Gardner, Milad Hashemi, Graham Neubig, Parthasarathy Ranganathan, Osbert Bastani, and Amir Yazdanbakhsh. 2024. Learning Performance-Improving Code Edits. arXiv:2302.07867 [cs.SE] <https://arxiv.org/abs/2302.07867>
- [67] William Thies, Frédéric Vivien, Jeffrey Sheldon, and Saman Amarasinghe. 2001. A unified framework for schedule and storage optimization. In *Proc. of the 2001 PLDI Conf.*
- [68] Konrad Trifunovic, Dorit Nuzman, Albert Cohen, Ayal Zaks, and Ira Rosen. 2009. Polyhedral-Model Guided Loop-Nest Auto-Vectorization. In *18th International Conference on Parallel Architectures and Compilation Techniques*. IEEE, Piscataway, NJ, USA, 327–337. doi:10.1109/PACT.2009.18
- [69] Mircea Trofin, Yundi Qian, Eugene Brevdo, Zinan Lin, Krzysztof Choromanski, and David Li. 2021. MLGO: A Machine Learning Guided Compiler Optimizations Framework. arXiv preprint arXiv:2101.04808. <https://arxiv.org/abs/2101.04808>
- [70] Ashish Vaswani, Noam Shazeer, Niki Parmar, Jakob Uszkoreit, Llion Jones, Aidan N. Gomez, Lukasz Kaiser, and Illia Polosukhin. 2017. Attention Is All You Need. In *Advances in Neural Information Processing Systems 30 (NIPS 2017)*, I. Guyon, U. V. Luxburg, S. Bengio, H. Wallach, R. Fergus, S. Vishwanathan, and R. Garnett (Eds.). Curran Associates, Inc., Red Hook, NY, USA, 5998–6008. <http://papers.nips.cc/paper/7181-attention-is-all-you-need.pdf>
- [71] S. VenkataKeerthy, Siddharth Jain, Anilava Kundu, Rohit Aggarwal, Albert Cohen, and Ramakrishna Upadrasta. 2023. RLReAl: Reinforcement Learning for Register Allocation. In *Proceedings of the 32nd ACM SIGPLAN International Conference on Compiler Construction (CC ’23)*. ACM, New York, NY, USA, 133–144. doi:10.1145/3578360.3580273
- [72] Alexander Viand, Patrick Jattke, Miro Haller, and Anwar Hithnawi. 2022. HECO: Fully Homomorphic Encryption Compiler. In *31st USENIX Security Symposium (USENIX Security 22)*. USENIX Association, Berkeley, CA, USA, 4133–4150. <https://www.usenix.org/conference/usenixsecurity22/presentation/viand>
- [73] Alexander Viand, Patrick Jattke, and Anwar Hithnawi. 2021. SoK: Fully Homomorphic Encryption Compilers. In *2021 IEEE Symposium on Security and Privacy (SP)*. IEEE, Piscataway, NJ, USA, 1092–1108. doi:10.1109/SP40001.2021.00068
- [74] Zheng Wang and Michael O’Boyle. 2018. Machine Learning in Compiler Optimization. *Proc. IEEE PP* (05 2018), 1–23. doi:10.1109/JPROC.2018.2817118
- [75] Zhongcheng Zhang, Ying Liu, Yuyang Zhang, Zhenchuan Chen, Jiacheng Zhao, Xiaobing Feng, Huimin Cui, and Jingling Xue. 2025. Qiwu: Exploiting Ciphertext-Level SIMD Parallelism in Homomorphic Encryption Programs. In *Proceedings of the 2025 IEEE/ACM International Symposium on Code Generation and Optimization (CGO)* (Las Vegas, NV, USA). ACM, New York, NY, USA, 523–537.
- [76] Lianmin Zheng, Chengfan Jia, Minmin Sun, Zhao Wu, Cody Hao Yu, Ameer Haj-Ali, Yida Wang, Jun Yang, Danyang Zhuo, Koushik Sen, Joseph E. Gonzalez, and Ion Stoica. 2020. Ansr: generating high-performance tensor programs for deep learning. In *Proceedings of the 14th USENIX Conference on Operating Systems Design and Implementation (OSDI’20)*. USENIX Association, USA, Article 49, 17 pages.